https://doi.org/10.5194/essd-2020-331
Preprint. Discussion started: 17 November 2020

Open Access Earth System Science Data Discussions

Measurements from the *RV Ronald H. Brown* and related platforms as part of the Atlantic Tradewind Ocean-Atmosphere Mesoscale Interaction Campaign (ATOMIC)

Patricia K. Quinn[1], Elizabeth Thompson[2], Derek J. Coffman[1], Sunil Baidar[3,4], Ludovic Bariteau[2], Timothy S. Bates[1,5], Sebastien Bigorre[6], Alan Brewer[4], Gijs de Boer[2,3], Simon P. de Szoeke[7], Kyla Drushka[8], Gregory R. Foltz[9], Janet Intrieri[2], Suneil Iyer[8], Chris W. Fairall[2], Cassandra J. Gaston[10], Friedhelm Jansen[11], James E. Johnson[1,5], Ovid O. Krüger[12], Richard D. Marchbanks[3,4], Kenneth P. Moran[2,3], David Noone[13], Sergio Pezoa[2], Robert Pincus[2,3], Albert J. Plueddemann[6], Mira L. Pöhlker[12], Ulrich Pöschl[12], Estefania Quinones Melendez[7], Haley M. Royer[10], Malgorzata Szczodrak[10], Jim Thomson[8], Lucia M. Upchurch[1,5], Chidong Zhang[1], Dongxiao Zhang[1,5], and Paquita Zuidema[10]

[1]NOAA Pacific Marine Environmental Laboratory (PMEL), Seattle, WA, USA
[2]NOAA Physical Sciences Laboratory (PSL), Boulder, CO, USA
[3]Cooperative Institute for Research in Environmental Sciences (CIRES), University of Colorado, Boulder, CO
[4]NOAA Chemical Sciences Laboratory (CSL), Boulder, CO, USA
[5]Cooperative Institute for Climate Ocean and Ecosystem Studies (CICOES), University of Washington, Seattle, WA, USA
[6]Woods Hole Oceanographic Institution (WHOI), Woods Hole, MA, USA
[7]Oregon State University, Corvallis, OR, USA
[8]University of Washington, Applied Physics Laboratory (APL), Seattle, WA
[9]NOAA Atlantic Oceanographic and Meteorological Laboratory (AOML), Miami, FL, USA
[10]Rosenstiel School of Marine and Atmospheric Science, University of Miami, Miami, FL, USA
[11]Max Planck Institute for Meteorology, Hamburg, Germany
[12]Max Planck Institute for Chemistry, Mainz, Germany
[13]University of Auckland, Auckland, NZ

Correspondence: Patricia K. Quinn (patricia.k.quinn@noaa.gov)

Abstract. The Atlantic Tradewind Ocean-Atmosphere Mesoscale Interaction Campaign (ATOMIC) took place from January 7 to July 11, 2020 in the tropical North Atlantic between the eastern edge of Barbados and 51°W, the longitude of the Northwest Tropical Atlantic Station (NTAS) mooring. Measurements were made to gather information on shallow atmospheric convection, the effects of aerosols and clouds on the ocean surface energy budget, and mesoscale oceanic processes. Multiple platforms were deployed during ATOMIC including the *NOAA RV Ronald H. Brown* (RHB) (Jan. 7 to Feb. 13) and WP-3D Orion (P-3) aircraft (Jan. 17 to Feb. 10), the University of Colorado's RAAVEN Uncrewed Aerial System (UAS) (Jan. 24 to Feb. 15), NOAA- and NASA-sponsored Saildrones (Jan. 12 to Jul. 11), and Surface Velocity Program Salinity (SVPS) surface ocean drifters (Jan. 23 to Apr. 29). The *RV Ronald H. Brown* conducted *in situ* and remote sensing measurements of oceanic and atmospheric properties with an emphasis on mesoscale oceanic-atmospheric coupling and aerosol-cloud interactions. In addition, the ship served as a launching pad for Wave Gliders, Surface Wave Instrument Floats with Tracking (SWIFTs), and radiosondes. Details of measurements made from the *RV Ronald H. Brown*, ship-deployed assets, and other platforms closely coordinated with the ship during ATOMIC are provided here. These platforms include Saildrone 1064 and the RAAVEN UAS as well as the Barbados Cloud Observatory (BCO) and Barbados Atmospheric

https://doi.org/10.5194/essd-2020-331
Preprint. Discussion started: 17 November 2020

Chemistry Observatory (BACO). Inter-platform comparisons are presented to assess consistency in the data sets. Data sets from the *RV Ronald H. Brown* and deployed assets have been quality controlled and are publicly available at the NOAA Physical Sciences Laboratory (PSL) ATOMIC ftp server (ftp://ftp2.psl.noaa.gov/Projects/ATOMIC/data/ (Quinn et al., 2020). In addition, the data have been submitted to NOAA's National Centers for Environmental Information (NCEI) data archive (https://www.ncei.noaa.gov/) for Digital Object Identifiers (DOIs). Point of contact information and links to individual data sets are provided herein.

1. Introduction

Shallow, liquid clouds persist at altitudes of hundreds to a few thousand meters above most of the world's oceans. Convection and mixing in the boundary layer can lead to the formation of shallow clouds, which can drive more mixing throughout the cloud layer and result in deeper convection. These clouds reflect incoming solar radiation and lead to a cooling of the surface (Vial et al., 2016). In addition, shallow mixing influences sea surface temperature (SST) and salinity by moderating the air-sea exchanges of energy and moisture (Stevens et al., 2016). Climate models have difficulty accurately representing low clouds in trade-wind regions because many of the processes involved in their formation occur at sub-grid scales (Bony et al., 2015). Improving model performance requires measurements that will result in a better understanding of 1) the boundary layer conditions that lead to cloudiness, 2) the influence of clouds and the atmospheric boundary layer on the upper ocean mixed layer, and in turn, 3) the influence of ocean mixing processes on surface fluxes and the atmospheric boundary layer.

ATOMIC took place in the boreal winter to study shallow convection and low, liquid clouds at a time of year when other cloud types are mostly absent. ATOMIC is the U.S. complement to the Elucidating the Role of Clouds Circulation Coupling in Climate Campaign (EUREC^{4}A) (Bony et al., 2017;Stevens et al., 2020). Together, ATOMIC and EUREC^{4}A involved 4 research vessels, 4 research aircraft, land-based observations from Barbados, and uncrewed sea-going and aerial vehicles. The ATOMIC - EUREC^{4}A study region stretched from the eastern shores of Barbados to the NTAS buoy located ~500 NM to the northeast and south along the coast of South America to ~ 5°N. EUREC^{4}A platforms focused on the western portion of the study area while the *RV Ronald H. Brown* and P-3 aircraft worked primarily in the eastern, upwind sector from mid-January to mid-February (Fig. 1). NOAA- and NASA-sponsored Saildrones covered the entire study area between January and July 2020. The RAAVEN UAS flew near shore from Morgan Lewis on the eastern side of Barbados between January 24 and February 15. SVPS type surface ocean drifters were deployed from the *RV L'Atalante* and operated along the South American coast (Jan. 23 to Apr. 29).

https://doi.org/10.5194/essd-2020-331
Preprint. Discussion started: 17 November 2020

Figure 1. Tracks of the *RV Ronald H. Brown* (colored by seawater skin T calculated by PSL), Wave Gliders, and SWIFTS during ATOMIC for a) Leg 1 and b) Leg 2. Shown in the insets for Legs 1 and 2 are the tracks of the 2 Wave Gliders (straight, light colored lines) and 6 SWIFTs (wavy, bold colored lines). The portion of the EUREC[4]A study area overlapping with ATOMIC is indicated by the solid green line in b). Locations of *RV Ronald H. Brown* stations, MOVE, and BCO/BACO are also shown.

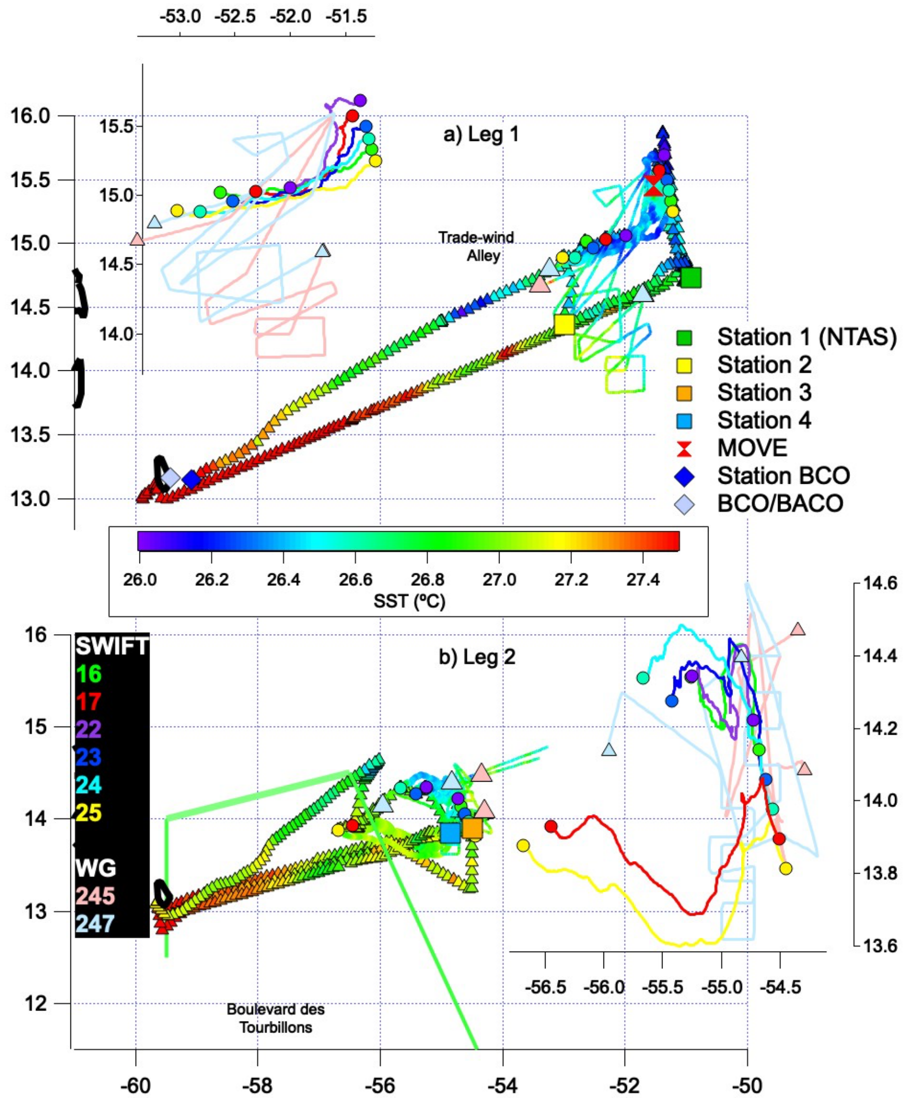

A thorough description of the objectives of ATOMIC and first highlights of the data analyses are presented in Zuidema (2020). A description of data collected from the P-3 is described in Pincus et al. (2020) and data collected by the RAAVEN are documented in de Boer et al. (2020). Here, a detailed overview of the data collected from the

RV Ronald H. Brown and deployed assets is provided. The goal is to document the sampling strategy, instrumentation used, and data availability to advance the widespread use of the data by the ATOMIC and broader research communities. A description of the sampling strategy, including coordination with other platforms, is described in Sect. 2. Also detailed in Sect. 2 are the measurements made from the *RV Ronald H. Brown,* the NTAS moored buoy, Wave Gliders and SWIFT vessels, Saildrones, RAAVEN UAS, and SVPS drifters. An overview of oceanic and atmospheric conditions sampled is provided in Sect. 3. Results from inter-platform comparisons of atmospheric and oceanic parameters are detailed in Sect. 4. Data availability, format, and quality control are described in Sect. 5 along with links to data sets.

2. Sampling strategy and measurements

Sampling onboard the *RV Ronald H. Brown* took place from Jan. 7 to Feb. 13, 2020 and focused on the region between 57°W and 51°W east of Barbados and between 13° and 16°N in the so-called Trade Wind Alley (Fig. 1). The overarching strategy of ATOMIC was to provide a view of the atmospheric and oceanic conditions upwind of the EUREC^{4}A study region. Operations of the *RV Ronald H. Brown* were coordinated with the Wave Gliders and SWIFTs deployed from the ship, the P-3 aircraft, Saildrone 1064, and BCO and BACO. An additional logistical objective included recovering the NTAS-17 mooring and replacing it with the NTAS-18 mooring. A third objective was to triangulate and download data from a Meridional Overturning Variability Experiment (MOVE) subsurface mooring and related Pressure Inverted Echo Sounders (PIES). MOVE is designed to monitor the integrated deep meridional flow in the tropical North Atlantic.

Optimal aerosol and flux measurements were made when the ship was pointed into the wind to avoid contamination by the ship's stack and air flow distortion. Coordinating with the P-3 and Saildrone and deploying the NTAS Mooring, Wave Gliders, and SWIFTs had the advantage of providing redundant and complimentary data streams but the disadvantage of requiring the ship to transit away from the wind for maneuvers. In addition, ship transits to Bridgetown for a scheduled in port (Jan. 26 to 28) and a medical emergency (Feb. 3 to 6) were downwind relative to prevailing northeast trade winds. Periods of unfavorable winds for atmospheric sampling were identified by relative winds abaft the beam (~ - 90° through 180° to + 90° relative to the bow) and high particle number concentrations as shown in Figure 2. Unfavorable sampling conditions were experienced 15% of the time the ship was at sea at the dates and times indicated in Table 1. Seawater measurements were less accurate when the ship's speed over water was near zero due to mechanical stirring of the water surface by the ship's propulsion system.

A general timeline of events for Legs 1 and 2 is provided in Sect. 2.1. and 2.2. Descriptions of the instrumentation onboard the ship and deployed assets are provided in Sect. 2.3 to 2.7 and on the Saildrone, RAAVEN UAS, and SVPS drifters in Sect. 2.8 to 2.10.

https://doi.org/10.5194/essd-2020-331
Preprint. Discussion started: 17 November 2020

Open Access Earth System Science Data Discussions

Figure 2. Time series of relative wind direction (apparent wind relative to the bow of the ship, negative values are port and positive values are starboard) and particle number concentration measured on the *RV Ronald H. Brown* during ATOMIC.

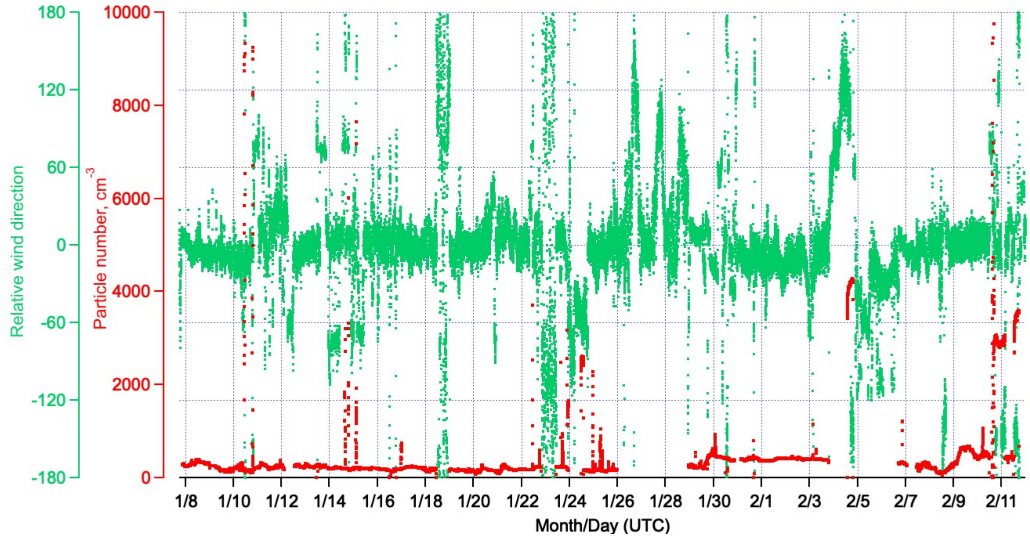

2.1. Sampling events during Leg 1

Timeline of events for Legs 1 and 2 are shown in Table 1. Dates and positions of deployment and recovery of assets are listed in Table 2. Times when platforms were within relatively close proximity providing the potential for inter-platform comparisons are given in Table 3. All times reported throughout the paper are in UTC.

The ship departed Bridgetown, Barbados on Jan. 7, 2020 in transit to the NTAS-18 mooring target location at 14°44'N and 50°56'W. Radiosonde launches every 4 hours and continuous atmosphere and sea surface sampling began early on Jan. 8. The latitude and longitude of the four stations occupied during the cruise are listed in Table 1 and shown in Figure 1. Station 1 (S1) was located in the NTAS region. Two Wave Gliders were deployed on Jan. 9 *en route* to S1. Once at S1, early on Jan. 10 a comparison between shipboard and NTAS-17 atmosphere and ocean measurements was conducted. The NTAS-18 mooring was deployed later on Jan. 10. After deployment, the ship transited 55 nm to the northwest of S1 to the MOVE region near 15°27'N and 51°32'W (Figure 1). Unsuccessful attempts were made over a 24 hr period to triangulate the position of the MOVE1-13 mooring and PIES198 and 238. The ship left the MOVE region on Jan. 12 at 05:30 to transit back to S1. The MOVE work did not compromise continuous atmospheric and surface ocean sampling and is not discussed further.

https://doi.org/10.5194/essd-2020-331
Preprint. Discussion started: 17 November 2020

Table 1. Timeline of sampling events onboard the *RV Ronald H. Brown* (RHB) including coordination with other platforms, NTAS operations, downwind transits, and periods on Station. The different colors shown under RHB correspond to the status of the ship. *NTAS-18 deployed. **NTAS-17 recovered.

	Sampling days
	Downwind transit
	In port
	NTAS Operations
	MOVE Operations
C-BCO	Comparison with BCO
C-P3 (Research Flight number)	Coordination with P3
C-SD	Comparison with SailDrone 1064
C-S	Comparison with SWIFTs
C-N17	Comparison with NTAS 17
C-N18	Comparison with NTAS 18
C-RUAS	Comparison with RAAVEN UAS
S1	Station 1 14°44' N, 50°56'W (NTAS area)
S2	Station 2 14°21'44"N, 53°W
S3	Station 3 13°54'N, 54°30'W
S4	Station 4 13°51'N, 54°51'36"W
Station BCO	Station BCO 13°8'55.7", 59°4'59.2"W

	RHB	SWIFTs	WG 245	WG 247	CTD	uCTD	NTAS/ MOVE
Jan 7							
8							
9	S1						
10	S1, C-N17						N18*
11							MOVE
12	S1, C-N18						
13	S1, C-N18, C-S						
14	C-S						
15	S1, C-N17						
16	S1, C-N17						N17**
17	S1, C-P3(RF1)						
18	C-P3 (RF2)						
19	S2						
20	S2						
21	S2						
22	C-S						
23	C-P3(RF3)						
24	C-BCO, C-RUAS						
25	C-BCO, C-RUAS						
26							
27							
28							
29							
30	C-S, S3						
31	S3, C-P3(RF5)						
Feb 1	S3						
2	S3						
3	S3, C-P3(RF6)						
4							
5							
6							
7							
8	S4, C-SD, C-P3(RF9)						
9	S4, C-SD						
10	S4, C-SD, C-P3(RF10)						
11	C-S, C-WG, C-P3(RF11)						
12							
13							

https://doi.org/10.5194/essd-2020-331
Preprint. Discussion started: 17 November 2020

Table 2. Dates (UTC) and positions of deployment and recovery of NTAS moorings, two Wave Gliders, and six SWIFTs. Assets are listed in order of start and stop times of the data stream. Distance travelled is given for the SWIFTs and Wave Gliders.

	Deployment		Recovery		
Asset	**Date**	**Position**	**Date**	**Position**	**Distance (nm)**
LEG 1					
Wave Glider 245	1/9/20 20:55	14° 35’ 25” N, 51° 41’ 56” W			
Wave Glider 247	1/9/20 20:55	14° 35' 13" N, 51° 42' 21" W			
NTAS-18	1/10/20 17:45	14° 44’ N, 50° 56’W			
SWIFT 22	1/14/20 01:13	15° 41' 21" N, 51° 22' 5" W	1/22/20 19:14	15° 3' 29" N, 51° 59' 50" W	52
SWIFT 23	1/14/20 05:11	15° 29' 59" N, 51° 18' 54" W	1/22/20 15:11	14° 57' 47" N, 52° 31' 21" W	62
SWIFT 24	1/14/20 07:11	15° 24' 42" N, 51° 17' 19" W	1/22/20 12:13	14° 53' 12" N, 52° 49' 5" W	94
SWIFT 16	1/14/20 9:11	15° 20' 3" N, 51° 15' 37"	1/22/20 14:13	15° 1' 9", 52° 38' 8"W	82
SWIFT 25	1/14/20 10:12	15° 15' 7" N, 51° 13' 46" W	1/22/20 11:13	14° 53' 26"N, 53° 1' 34" W	60
SWIFT 17	1/14/20 18:11	15° 34' 31" N, 51° 26' 16" W	1/22/20 17:14	15° 1' 55" N, 52° 18' 56" W	60
NTAS-17			1/16/20 10:41	14° 49’ 28” N, 51° 00’ W	
LEG 2					
Wave Glider 245			2/7 19:55	14° 4’ 55” N, 54° 17’ 12” W	153
SWIFT 22	1/30/20 17:12	14° 13' 25" N, 54° 43' 53" W	2/10/20 17:12	14° 20' 35" N, 55° 15' 5" W	31
SWIFT 16	1/30/20 18:13	14° 8' 23" N, 54° 40' 51" W	2/10/20 17:13	14° 20' 28" N, 55° 15' 19" W	36
SWIFT 23	1/30/20 19:12	14° 3' 31" N, 54° 37' 30" W	2/10/20 20:15	14° 16' 30" N, 55° 25' 14" W	48
SWIFT 24	1/30/20 20:13	13° 58' 39" N, 54° 33' 52" W	2/10/20 23:12	14° 20' 19" N, 55° 39' 56" W	68
Wave Glider 247			2/11/20 10:54	14° 8’ 11” N, 55° 57’ 9” W	248
SWIFT 17	1/30/20 21:10	13° 53' 40" N, 54° 30 '31" W	2/11/20 15:11	13° 55' 47" N, 56° 27' 6" W	127
SWIFT 25	1/30/20 22:13	13° 48' 50" N, 54° 27' 6" W	2/11/20 17:14	13° 52' 37" N, 56° 41' 0.6" W	130

Table 3. Times when platforms were within relatively close proximity providing the potential for inter-platform comparisons. Also given are distances between platforms during the comparisons. Results from inter-platform comparisons reported here are indicated in bold. Distances between RHB and NTAS refer to distance to the mooring anchor. Distance to buoys were between 0.25 to 3 NM.

Platforms	Start UTC	Stop UTC	Distance (nm)	Comments
RHB, NTAS-17	1/10/20 00:58	1/10/20 08:57	2.5 (mooring anchor)	Station 1
RHB, NTAS-18	**1/12/20 11:30**	**1/13/20 14:00**	**2.9 (mooring anchor)**	**1/12/20 14:06, 19:04; 1/13/20 00:00 CTD casts to 250 m Station 1**
RHB, NTAS-17	**1/15/20 10:00**	**1/16/20 09:05**	**2.9 (mooring anchor)**	**1/15/20 20:16 CTD cast to 5000 m Station 1**
RHB, P-3	1/17/20 14:20		Within dropsonde circle	P-3 RF1, 7.3 – 7.7 km altitude Station 1
RHB, P-3	1/19/20 14:57		Within dropsonde circle	P-3 RF2 7.6 km altitude Station 2
RHB, P-3	1/23/20 14:06, 19:46		Within dropsonde circle	P-3 RF3, 3.2 km altitude 14° 22' 59”N and 55°W Overfly of ship at 150 m at 15:42
RHB, P-3	1/31/20 16:25		Within dropsonde circle	P-3 RF5, 7.4 km altitude Station 3
RHB, P-3	2/3/20 14:13		Within dropsonde circle	P-3 RF6, 7.7 km altitude Station 3
RHB, P-3	2/9/20 05:57		Within dropsonde circle	P-3 RF9, 7.5 km altitude Station 4
RHB, P-3	2/10/20 05:46		Within dropsonde circle	P-3 RF10, 7.5 km altitude Station 4
RHB, P-3	2/11/20 10:26			P-3 RF11, 7.5 km altitude Station 4
RHB, SD 1064	**2/8/20 9:30**	**2/10/20 18:50**	**0.7 to 3.6**	**2/8/20 9:30 – 18:10 SD was 2.8 – 3.6 NM upwind, 2/8 19:00 0 2/10 18:50 SD was 0.7 – 0.8 NM from ship Station 4**
RHB, BCO	**1/24/20 18:20**	**1/25/20 23:40**	**20**	**RHB located directly upwind of BCO**

https://doi.org/10.5194/essd-2020-331
Preprint. Discussion started: 17 November 2020

A comparison of atmospheric and oceanic parameters measured onboard the ship and NTAS-18 was conducted Jan. 12 to 13. The comparison included a CTD (conductivity, temperature, and depth) sensor mounted on the ship's rosette and conductivity and temperature sensors attached to the NTAS mooring line. While waiting for the weather to calm down enough to recover NTAS-17, 6 SWIFTs were deployed. The ship transited 55 NM to the northwest and deployed the first SWIFT (22) on Jan. 14 at 01:13 UTC at 15° 41' 21" N, 51° 22' 5" W (Fig. 1, Table 2). Following a southeast track, the remaining 5 SWIFTs were deployed 5 to 12 nm apart across horizontal gradients in ocean surface current and temperature. SWIFT17, the second one deployed, was recovered due to the failure of a 3-D sonic anemometer. The ship returned to SWIFT17 to swap out the anemometer. It was re-deployed near its original position on Jan. 14 at 18:11 UTC. After each SWIFT deployment, underway CTD (uCTD) casts were performed to a depth of 50 m for comparison to SST and salinity measured onboard the SWIFTs and to understand the ocean mixed layer structure at the beginning of each SWIFT Lagrangian drift. In addition, the ship sat near each SWIFT for at least an hour after deployment for a comparison of measured near surface atmospheric and surface sea water parameters.

The ship returned to S1 and conducted a second comparison with NTAS-17 on Jan. 15 to 16, including a CTD cast with the ship's rosette and sensors on the NTAS mooring line. NTAS-17 was recovered on Jan. 16. The ship stayed at S1 and was within the P-3's dropsonde circle during its first flight (Research Flight 1 or RF1) on Jan. 17 from 15:30 to 16:40. A first comparison between the uCTD and the CTD on the ship's rosette for temperature and salinity was conducted on Jan. 17 at 22:36. The ship's CTD cast went to a depth of 500 m.

With the NTAS and MOVE work finished, the ship transited downwind on Jan. 18 for 14.5 hours to Station 2 (S2) located at 14º21'44"N and 53ºW (Fig. 1a). This location was downwind of the projected paths of the SWIFTs but still upwind of the EUREC^{4}A study region. During the transit, aerosol and flux measurements were compromised by relative winds abaft the beam but surface ocean and meteorological measurements as well as radiosonde launches continued. In addition, uCTD casts to 100 m depth were made every hour to investigate a large-scale SST gradient between NTAS and S2. The ship briefly slowed to 2 to 4 kts for each cast.

The ship reached S2 on Jan. 19 at 01:30 UTC and turned into the wind for optimal aerosol and flux measurements. Underway CTDs were conducted to a depth of 100 m every 6 hr. The second overflight of the P-3 (RF2) occurred on Jan. 19 at 14:57 UTC with the *RV Ronald H. Brown* within the aircraft's dropsonde circle. A second comparison between the uCTD and the CTD on the ship's rosette was conducted on Jan. 21 at 16:15 with the ship's CTD reaching a depth of 150 m.

On Jan. 22 at 07:30 UTC, the ship left S2 to recover the SWIFTs before the end of Leg 1. The SWIFTs had drifted between 53 and 103 NM to the southwest with those deployed at the more southern locations drifting the furthest (Fig. 1a, Table 2). The ship transited 32 NM to the north to reach the southernmost SWIFT and then followed a course to the northeast recovering the remaining SWIFTs which were 7 to 24 NM apart. Once all SWIFTs were

https://doi.org/10.5194/essd-2020-331
Preprint. Discussion started: 17 November 2020

onboard (Jan. 22 19:14), the ship transited 180 NM to the southwest to 14° 22' 59"N and 55°W to be in the center of the P-3's dropsonde circle the next day. Aerosol and flux measurements were compromised during the transit due to the relative wind being abaft the beam.

The ship reached the designated position on Jan. 23 at 10:30, turned into the wind for optimal aerosol and flux measurements, and was within the P-3's dropsonde circle on Jan. 23 at 14:06 (RF3). Later in the flight (15:42), the P-3 flew over the ship at an altitude of 150 m. This flyby was the closest the P-3 was to the ship during the ATOMIC campaign while all instrumentation was operational. At 22:00 the ship started the 250 NM transit back to Bridgetown with a planned stop upwind of BCO/BACO for a measurement comparison. Initially, relative winds were from the port side of the ship at -100° relative to the bow but 6 hrs into the transit they shifted to a relative direction of -50° due to a change in true wind direction and the ship's course, making for better conditions for aerosol and flux measurements. Radiosonde launches were halted on Jan. 24 at 2:45 near 56°W with the knowledge that sondes launched from the *RV Meteor* and BCO could be used to fill in the gap. The ship arrived at the comparison point 20 NM east of BCO (13° 8' 55.7"N, 59° 4' 59.2"W) at 18:20 on Jan. 24 and stayed until Jan. 25 at 23:40 (Fig. 1a). Underway CTDs were conducted approximately every 2 hours until Jan. 25 at 21:58.

The ship ended Leg 1 with a transit around the southern end of Barbados and into Bridgetown with an arrival on Jan. 26 at 12:15.

2.2. Sampling events during Leg 2

The *RV Ronald H. Brown* left Bridgetown at 22:15 on Jan. 28 and headed for Station 3 (S3) located 290 NM to the northeast of BCO/BACO at 13° 54' 0"N and 54° 30' 0"W (Fig. 1a). S3 was roughly halfway between BCO/BACO and NTAS. Radiosonde launches began on Jan. 29 at 6:45 and continued every 4 hrs. The ship veered off its NE track on Jan. 29 at 20:18 and turned to the southeast to map the spatial orientation of SST fronts for determining where to deploy SWIFTs. When done with mapping, the ship went north on Jan. 30 at 4:15 arriving in the vicinity of S3 and Wave Glider 245 at 08:00. Wave Glider 245 was recovered to replace malfunctioning sensors.

The ship zigzagged to the northwest and then northeast until reaching 14° 13' 25" N and 54° 43' 53" W on Jan. 30 at 17:12 where the first SWIFT deployment of Leg 2 took place (Fig. 1b, Table 2). The remaining SWIFTs were deployed on a southeast track approximately 6 NM apart. After each SWIFT deployment, uCTD casts were performed to a depth of 100 m to provide a subsurface context for SWIFT measurements. During each cast, the ship moved into the wind at 0.5 kts. Wave Glider 245 was re-deployed on Jan. 30 at 18:08 after the last SWIFT was put in the water. The ship then transited back to S3, arriving 5 hrs later at 23:09. During this 6 hr period, as the ship was maneuvering to deploy SWIFTs, relative winds were from the port side between -50 to -100 degrees compromising aerosol and flux measurements.

https://doi.org/10.5194/essd-2020-331
Preprint. Discussion started: 17 November 2020

The ship remained at S3 until Feb. 3 at 15:00 making continuous atmospheric and surface ocean measurements, launching radiosondes every 4 hrs, and conducting uCTD casts every 2 hrs. Four comparisons between the uCTD and the CTD on the ship's rosette were conducted between Feb. 1 and Feb. 3 with the ship's CTD reaching a depth of 400 m. The ship was at the center of the P-3's dropsonde circle on Jan. 31 at 16:25 (RF5) and Feb. 3 at 14:13 (RF6).

On Feb. 3 at 19:30 the ship headed back to Bridgetown for a medical emergency. Aerosol and flux measurements were compromised due to relative winds abaft the beam. Radiosonde launches continued every 4 hours. The last launch before reaching port was on Feb. 4 at 10:45. The ship arrived in Bridgetown on Feb. 4 at 19:00.

The ship departed Bridgetown on Feb. 6 at 16:00 and headed northeast to Station 4 (S4) located at 13º51'N and 54º51'36"W, 21.2 NM southwest of S3. Atmospheric measurements resumed along with radiosonde launches every 4 hrs. The ship arrived at S4 on Feb. 8 at 01:00 but left 6 hrs later to recover Wave Glider 245 because it was experiencing navigation problems that could have endangered the vehicle. The Wave Glider was recovered 36 NM to the northeast of S4 (14° 4' 55" N, 54° 17' 12" W) on Feb. 8 at 12:45. Aerosol and flux measurements were compromised during the downwind transit back to S4 between 12:45 and 16:25. Once back on station, optimal aerosol and flux measurements resumed along with uCTD casts every 2 hrs. A CTD cast to a depth of 1000 m with the ship's rosette was conducted on Feb. 8 at 17:00 for comparison to the uCTD.

Still at S4, the ship was within the P-3's night time dropsonde circle on Feb. 9 (RF9) at 5:57. The NOAA PMEL-operated Saildrone 1064 completed a first leg between BCO and NTAS and then sailed near the ship for a comparison of fluxes and measured meteorological and seawater parameters. The Saildrone was 2.8 to 3.6 NM upwind of the ship between Feb. 8 from 9:30 to 18:10 and within 0.7 to 0.8 NM of the ship between Feb. 8 19:00 and Feb. 10 18:50. Two final comparisons between the uCTD and the CTD on the ship's rosette were conducted on Feb. 8 and Feb. 9 with the ship's CTD going to depths of 1000 and 400 m, respectively. The ship remained at S4 for the P-3's second night flight (RF10) and was within the dropsonde circle on Feb. 10 from 05:46 to 06:42. The ship's final coordination with the P-3 occurred during a combination research and sightseeing flight with press (RF11) on Feb. 11. The ship was not within the dropsonde circle but was flown over at sunrise at 10:26.

The ship remained at S4 until Feb. 10 at 12:00 at which point aerosol measurements were ended and the ship began the transit to recover SWIFTs and Wave Glider 247. Recovery operations were conducted between Feb. 10 15:00 and Feb. 11 18:15. The four SWIFTs (16, 22, 23, and 24) that were initially deployed to the north between 14° 13' 25" and 13° 58' 39" N drifted to the northwest travelling a total distance ranging from 31 to 68 NM (Table 2, Fig. 1b). The two SWIFTs (17 and 25) deployed to the south between 13° 53' 40" N and 13° 48' 50" N initially drifted to the southwest, each traveling 130 nm. The ship transited to the northeast to pick up the northern cluster of SWIFTs first, staying near each asset for up to 1.5 hrs for a comparison of measured atmospheric and oceanic parameters.

https://doi.org/10.5194/essd-2020-331
Preprint. Discussion started: 17 November 2020

Open Access Earth System Science Data Discussions

The ship then did several back-and-forth tracks between the position of Wave Glider 247 and SWIFT 17 mapping a SST front before recovering the Wave Glider and the last two SWIFTs.

After the SWIFTs and Wave Glider were recovered, the ship started a northeast transit on Feb. 11 around 19:30 across a SST front in the upwind direction to study air-sea interaction and atmospheric and oceanic mixed layer variability. Underway CTDs were made continuously. On Feb. 12 at 06:00, the ship began the southwest transit back to Bridgetown for the final time. Atmospheric sampling was compromised during the downwind transit. The last radiosonde launch occurred on Feb. 12 at 10:45. The ship arrived in port on Feb. 13 at 10:00.

2.3. NTAS operations and measurements

NTAS was established to provide accurate air-sea flux estimates and upper ocean measurements in a region with strong SST anomalies and the likelihood of significant local air-sea interaction on interannual to decadal timescales (Weller, 2018;Bigorre and Galbraith, 2018). The station is maintained at a site near 15°N and 51°W through successive mooring turnarounds. During Leg 1, the Upper Ocean Processes Group of the Woods Hole Oceanographic Institution (WHOI) and crew of the *RV Ronald H. Brown* deployed the NTAS-18 mooring and recovered the NTAS-17 mooring at nearby sites. Both moorings used Surlyn foam buoys as the surface element. These buoys are outfitted with two Air–Sea Interaction Meteorology (ASIMET) systems (Colbo and Weller, 2009). The ASIMET system measures, records, and transmits via Iridium satellites the surface meteorological variables necessary to compute air–sea fluxes of heat, moisture and momentum. The upper 160 m of the mooring line are outfitted with oceanographic sensors for the measurement of temperature, salinity and velocity. Information on the instruments providing real-time data, measured atmospheric and oceanic parameters, and height/depth of the measurements on the NTAS mooring are provided in Table 4.

Table 4. Instrumentation providing real-time data onboard the NTAS mooring.

Instrument	Measured/derived quantities, raw sampling interval	
	Atmospheric parameters	**Height (m)**
ASIMET system	Bulk air-sea fluxes, relative humidity, temperature, pressure, wind speed and direction, precipitation rate, longwave radiation, shortwave radiation, 1 min	3
	Oceanic parameters	**Depth (m)**
ASIMET system	Sea surface temperature and salinity, 1 min	0.8
Seabird (SBE-37 IM)	Temperature and salinity, 5min	10
NORTEK Aquadopp	Currents, 20 min	13
Seabird (SBE-37 IM)	Temperature and salinity, 5min	25
Seabird (SBE-37 IM)	Temperature and salinity, 5min	40
Seabird (SBE-37 IM)	Temperature and salinity, 5min	55
Seabird (SBE-37 IM)	Temperature and salinity, 5min	70

ASIMET data are sampled and recorded internally every minute. The oceanographic measurements are recorded either every 5 min or 10 min for temperature and salinity (depending on the instrument type) and 20 min or 1 hr for

https://doi.org/10.5194/essd-2020-331
Preprint. Discussion started: 17 November 2020

currents. The NTAS-18 mooring was deployed on Jan. 10 at 14° 44' N, 50° 56' W with anchor drop at 17:45 in 5055 m of water. The NTAS-17 mooring was recovered on Jan. 16 with anchor release at 10:41. Both buoys have a watch circle of about 2 NM from their respective anchors and were separated by about 6 NM during the January 10 to 16 period allowing for comparisons of measured ocean and atmosphere parameters. Atmospheric data from NTAS-17 and NTAS-18 were combined for comparison to measurements onboard the *RV Ronald H. Brown* (Sect. 4.2.1).Wind speed, air temperature, and specific humidity were adjusted to a height of 10 m and neutral atmospheric stability using the COARE 3.6 bulk model for the comparison (Fairall et al., 2003;Edson et al., 2013). NTAS data in the ATOMIC archive only include data collected during the ATOMIC campaign.

On Apr. 8, 2020 at 08:00 UTC, the NTAS-18 buoy went adrift. It meandered slowly toward the Caribbean for 7 months until being recovered on Oct. 20, 2020. NTAS-19 was deployed on Oct. 22, 2020.

2.4. Shipboard atmospheric measurements

Instrumentation onboard the *RV Ronald H. Brown* for the measurement of atmospheric and aerosol parameters is listed in Table 5. Locations of instruments on deck are shown in Figure 3. NOAA's Physical Science Laboratory (PSL) collected data to enable a deeper understanding and quantification of cloud processes, the environments in which they either grow or dissipate, how the ocean and atmosphere interact, and the spatial variability of these processes. Instrumentation mounted on the bow mast and forward O2 deck (two levels above the main deck) measured sea-surface meteorological properties, rain rate, radiative fluxes, and air-sea turbulent fluxes using bulk, eddy covariance, and inertial dissipation methods (Fairall et al., 1997;Fairall et al., 1996;Fairall et al., 2003;Edson et al., 2013). Vertical profiles of backscatter from a ceilometer mounted on the forward O3 deck (three levels above the main deck) provided cloud base height and temporal cloud fraction. For comparison with other platforms (NTAS and Saildrone 1064), wind speed, air temperature, air pressure, and specific humidity were adjusted to a height of 10 m using the COARE 3.6 bulk algorithm. Final data products of meteorological and navigation data are 1-min and 10-min averages of high-resolution raw data (see Table 5 for raw sampling intervals). The data are time-stamped at the beginning of the 1- and 10-min period. Fluxes were calculated at 10-min resolution, then interpolated to 1-min.

University of Miami (UM) provided high resolution measurements of cloud and rain to better understand the relationship between cloud properties and cloud spatial organization as a function of cloud mesoscale organization, in particular rain and the associated atmospheric cold pools (Stevens et al., 2020;Zuidema et al., 2012). Two collocated Parsivel disdrometers mounted on the forward O3 deck provided precipitation intensity, drop number, and equivalent radar reflectivity. A sky camera provided a 50° field of view oriented horizontally off the starboard side of the ship every 4 sec. A microwave radiometer was deployed to provide cloud liquid water path estimates but its data acquisition was unsuccessful and no data are available A Marine Atmospheric Emitted Radiance Interferometer (M-AERI) was mounted on the port side O2 deck rail (2 levels above the main deck) (Minnett et al., 2001). It measured the spectra of infrared emission from the sea surface and atmosphere for the derivation of skin

https://doi.org/10.5194/essd-2020-331
Preprint. Discussion started: 17 November 2020

Open Access Earth System Science Data Discussions

Table 5. Instrumentation onboard the *RV Ronald H. Brown* for the measurement of atmospheric and aerosol parameters. The O2 and O3 decks were two and three levels above the main deck, respectively. [a]Aerosol inlet was located on the O2 deck, 18 m.a.s.l. Final data products of meteorological and navigation data are 1-min and 10-min averages of high-resolution raw data and time-stamped at the beginning of the 1- and 10-min period. Fluxes were calculated at 10-min resolution, then interpolated to 1-min for those files.

Instrument	Measured/derived quantities, raw sampling interval	Location
	Atmospheric parameters	
Gill WindMaster Pro 3-axis ultrasonic anemometer	Wind vector, stress, and sensible heat flux, 0.1 sec	Bow mast
Optical precipitation sensor, OSI Inc., ORG-815 DA	Rain rate, 5 sec sampling, collected/recorded every 1 min	Bow mast
Li-COR 7500 Gas Analyzer	Water vapor density, turbulent latent heat flux, 0.1 sec	Bow mast
Vaisala HMT335	Air temperature, humidity, 1 min	Bow mast
Vaisala PTB220	Atmospheric pressure, 1 min	O2 deck
2 Eppley PSPs (Pyranometer)	Shortwave radiation, 1 min	O2 deck
2 Eppley PIRs (Pyrgeometer)	Longwave radiation, 1 min	O2 deck
Systron and Donner MP-1 6-axis motion detector system	3-D ship acceleration, 0.1 sec	Bow mast
Vaisala CL31 Ceilometer	Vertical profiles of backscatter from refractive index gradients, cloud base height, cloud fraction, 15 sec sampling from 0-7.7 km with 10 m vertical spacing	O3 deck
2 Parsivel optical rain gauges, 650 and 780 nm	Rain rate, equivalent radar reflectivity, particle number	O3 deck
StarDot Camera, NetCam XL	Pointed to starboard, field of view of 50°, image captured every 4 sec	O3 deck
Doppler lidar λ=1.5 μm	Atmospheric vertical velocity and backscatter intensity, horizontal wind profiles, estimates of cloud base and mixed layer heights; 0.5 sec	O2 deck
W-band (95.56 GHz) Doppler vertically pointing cloud radar	Vertical profiles of non-precipitating and lightly-precipitating clouds from 100 m to 4.2 km with 30 m vertical resolution every 0.5 sec	O2 deck
Dual-flow, two filtered radon detector	^{222}Rn, 30 min	O3 deck
Vaisala WXT536	T, RH, rain rate; 1 sec	O2 deck
Picarro water vapor isotope analyzer (L2130-fi)	Water vapor concentration and isotopic composition, 0.2 sec	Aerosol inlet[a]
Vaisala RS-41 radiosondes	Profiles of T, RH, P, and winds every 4 hrs	Main deck
Thermo Environmental Model 49C	Ozone, 1 sec	Inlet at 18 m.a.s.l.
	Aerosol Properties	
Collection with multi-jet cascade impactors and analysis by ion chromatography, thermal-optical, gravimetric, and XRF analysis	Size segregated concentrations of Cl^-, NO_3^-, $SO_4^=$, methanesulfonate (MSA^-), Na^+, NH_4^+, K^+, Mg^{+2}, Ca^{+2}, organic carbon, elemental carbon, trace elements; hours	Aerosol inlet[a]
DMPS and TSI 3321APS	Number size distribution 0.02 to 10 μm, 5 min	Aerosol inlet[a]
TSI 3025A, 3760A, 3010	Number concentration > 3, 13, 13 nm; 1 sec	Aerosol inlet[a]
TSI 3563 Nephelometer	Sub-1.1 and sub-10 μm light scattering and backscattering; 450, 550, 700 nm; 60% RH; 1 sec	Aerosol inlet[a]
TSI 3563 Nephelometers	Sub-1.1 μm scattering f(RH); 450, 550, 700 nm; dry and 80%RH; 1 sec	Aerosol inlet[a]
Radiance Research PSAP	Sub-1.1 and sub-10 μm light absorption; 467, 530, 660 nm; dry	Aerosol inlet[a]
DMT CCNC	Sub-1.1 μm cloud condensation nuclei concentration, 0.1 to 0.6% S, 1 sec	Aerosol inlet[a]
Solar Light Microtops Sunphotometer	Aerosol Optical Depth; 380, 440, 500, 675, 870 nm	O3 deck

https://doi.org/10.5194/essd-2020-331
Preprint. Discussion started: 17 November 2020

Figure 3. Instrumentation onboard the *RV Ronald. H. Brown* for the measurement of atmospheric and oceanic parameters located on a) the bow mast and forward O2 deck and b) port side O3 deck. Asset deployments are shown for c) NTAS mooring, d) ship's rosette with CTD and Niskin bottles, e) uCTD, f) SWIFT, g) Wave Glider, and h) radiosonde. Also shown are i) P-3 fly over of the ship on Jan. 23 and j) Saildrone upon its return to the U.S. (Newport, RI) from Barbados. Not shown are disdrometers on the port O3 deck and camera on the starboard O3 deck.

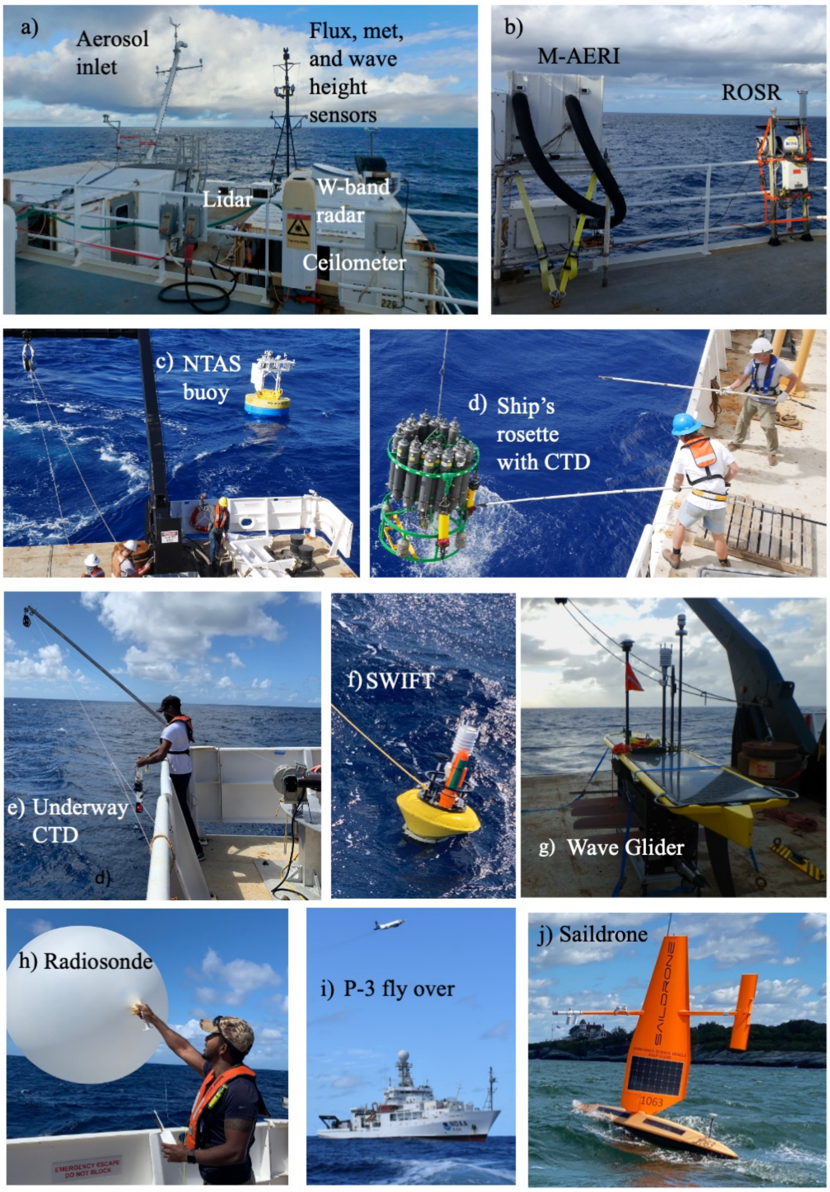

https://doi.org/10.5194/essd-2020-331
Preprint. Discussion started: 17 November 2020

sea surface temperature and lower troposphere profiles of temperature and humidity (Szczodrak et al., 2007). A W-band Doppler vertically pointing cloud radar was housed in a container on the O2 deck for the measurement of vertical profiles of non-precipitating and lightly-precipitating clouds (Moran et al., 2012). The radar was not functional during Leg 1 and operated with a 10 dB attenuator on Leg 2 that prevented detection of non-precipitating clouds.

NOAA's Chemical Sciences Laboratory (CSL) operated a microjoule class, pulsed Doppler lidar (microDop) operating at a wavelength of 1.5 µm to assess atmospheric turbulence, aerosol backscatter intensity, and horizontal winds (Schroeder et al., 2020). The lidar was mounted on the forward O2 deck. The system was motion stabilized while staring vertically to within 0.25 degrees of zenith. Ship motion projected onto the line-of-site velocity measurement was estimated and removed using a 6-axis inertial navigation unit (INU). The INU allowed the lidar to measure the mean and turbulent motions of aerosol in clear air and cloud scatterers with a spatial and temporal resolution of 33.6m and 2Hz respectively. The first valid gate was 75m above the ocean surface. The lidar pointed vertically 95% of the time to sample updrafts and downdrafts in the subcloud mixed layer and in the interstitial trade cumulus boundary layer and spent 2 minutes of every hour performing a 65° elevation, full azimuthal scan to measure horizontal wind profiles. Real-time quicklooks of backscatter intensity profiles showing strongly scattering cloud base and updraft structures were available for awareness of the clouds and turbulent mixed layer throughout the cruise. Cloud base height (CBH) was retrieved by applying Haar wavelet covariance transforms to the backscatter intensity profiles.

Oregon State University and the National Center for Atmospheric Research (NCAR) operated a Picarro water vapor isotope analyzer on Leg 2 of the cruise to investigate processes that shape the atmosphere's humidity structure and its variations. The spectroscopic analyzer measured water vapor concentration and its isotopic composition, the isotope ratios of oxygen ($^{18}O/^{16}O$) and hydrogen (D/H). All three quantities were measured continuously at 5 Hz frequency via the aerosol inlet on the O2 deck at 18 m above sea level (m.a.s.l.). Complementary gas-phase water isotopic measurements were made from the P-3, at BCO, from the French ATR aircraft, and aboard German and French research vessels. Rainwater and seawater were also collected from the ship platforms for future offline analysis. Surface sea water and water column samples from CTD casts were also collected to investigate the upper ocean mixing and the freshwater balance to be evaluated in the context of air-sea gas exchange and upper ocean circulation.

The goals of NOAA's Pacific Marine Environmental Laboratory (PMEL) were to assess the impact of aerosol-cloud interactions and direct aerosol light scattering and absorption on the temporal variability of net radiation reaching the ocean surface and SST. Measurements included aerosol chemical composition, total number concentration, number size distribution, light scattering and its dependence on relative humidity, light absorption, and cloud nucleating ability. Aerosol instrumentation was housed in two containers on the O2 deck. All instruments drew sample air from an inlet 18 m.a.s.l. mounted on top of one of the O2 deck vans (Bates et al., 2002) (Fig. 3). Aerosol optical depth (AOD) was measured using Microtops hand held sunphotometers. The raw Microtops data were processed by the NASA Maritime Aerosol Network in conjunction with the Aerosol Robotic Network (Smirnov et al., 2009). In addition, ^{222}Rn was measured for its use as a tracer of continentally-influenced air masses (Whittlestone and Zahorowski, 1998) and O_3 was measured for its use as an indicator of entrainment from the upper troposphere.

Radiosondes were launched throughout the ATOMIC campaign to provide information about the temporal evolution and vertical structure of the boundary layer, upper atmosphere, and clouds. A total of 97 radiosondes (Vaisala RS41-SGP) were launched from the fantail during Leg 1 and 66 were launched during Leg 2. There were 6 launches per day at 02:45, 06:45, 10:45, 14:45, 18:45, and 22:45 UTC. Vertical profiles of pressure, temperature, relative humidity, and winds were measured from the surface to approximately 25 km. Measurements were also made during the radiosondes' descent. Data were communicated to the Global Telecommunications System (GTS) following each sounding via email to the U.S. National Weather Service and via FTP to MeteoFrance. The data were reprocessed, gridded, and harmonized with all of the EUREC^{4}A sondes. Raw (Level-0), quality-controlled 1-second (Level-1), and vertically gridded (Level-2) data in NetCDF format are available to the public at AERIS (https://doi.org/10.25326/62). The methods of data collection and post-processing can be found in (Stephan et al., 2020).

Radiosonde operations were suspended on the ship west of ~56°W when the ship transited to Bridgetown for the planned in port (Jan. 24 at 2:45) and an emergency medical evacuation (Feb. 4 at 10:45). Soundings from BCO were stitched together with those from the ship to allow for an uninterrupted data record over the entire cruise.

The Lifted Condensation Level (LCL) was calculated from the BCO-RHB radiosonde data record and assumed to represent Cloud Base Height (CBH). The LCL (in m) was calculated as

$$LCL = (T_{50} - T_{d,50}) \times 125 + 50 \quad (1)$$

where T_{50} is temperature and $T_{d,50}$ is dew point, both at 50 m height (Espy, 1836;Bolton, 1980). The lowest altitude considered was 50 m to avoid contamination by the temperature and relative humidity near the ship's deck and to minimize the effect of vertical gradients in the surface layer. Since the calculation started at 50m, 50 was added to the LCL.

2.5. Shipboard oceanic measurements

Instrumentation onboard the *RV Ronald H. Brown* for the measurement of oceanic parameters is listed in Table 6. Locations of instruments mounted on the deck are shown in Figure 3. As stated above, UM's M-AERI, located on the port side forward O2 deck, measured sea surface skin temperature (Minnett et al., 2001).

Table 6. Instrumentation onboard the *RV Ronald H. Brown* for the measurement of seawater parameters. O2 deck is two levels above the main deck.

Instrument	Measured /derived quantities, raw sampling interval	Location
Marine Atmospheric Emitted Radiance Interferometer (M-AERI)	Sea surface skin temperature, 5 – 7 min averages	O2 deck
Remote Ocean Surface Radiometer (ROSR)	Sea surface skin temperature, 5 min averages	O2 deck
Floating YSI 46040 Thermistor (Sea snake)	Sub-skin sea surface temperature, ~ 0.05 m depth, 1 sec	Deployed off port side with outrigger
Riegl 1-D laser altimeter	Wave height and period, 10 min averages	Bow mast
Seabird 9+ CTD	At station conductivity (salinity), temperature, depth (pressure), PAR, fluorescence, and oxygen	Deployed off starboard side, main deck
Seabird SBE45 thermosalinigraph Seabird SBE38 thermistor	Seawater temperature, conductivity (salinity), 1 sec	5.3 m below the surface
Acoustic Doppler Current Profiler 75 kHz (ADCP)	Current velocity across 2 depth ranges depending on mode. Narrowband: 29-892 m. Broadband: 17-333 m. 5 min sampling.	Ship's hull
RBR Concerto underway CTD + Tuna Brute winch (uCTD)	Conductivity (salinity), temperature, and depth (pressure) from the surface to 60 or 130 m depending on cast	Deployed off starboard aft quarter

During Leg 1, the Applied Physics Laboratory at the University of Washington (APL-UW) also measured sea surface skin temperature with a Remote Ocean Surface Radiometer (ROSR) located near the M-AERI. PSL measured sub-skin temperature at approximately 0.05 m depth with a floating thermistor (a.k.a sea snake) deployed off the port side. A skin temperature value was estimated by the COARE algorithm using the sea snake data as input (Fairall et al., 1996;Fairall et al., 1997). This algorithm accounts for the cool skin present in the upper ~0.2-1 mm and any potential diurnal warm layers in the upper ~10 m. This COARE-calculated skin T and the current-relative wind were used to compute bulk, eddy covariance, and inertial dissipation air-sea fluxes (Fairall et al., 1997;Fairall et al., 2003). The COARE 3.6 algorithm estimated wave parameters using wind as input. The parameterization is based on fits to the Banner and Morison (2010) wave model and the flux database collected by NOAA PSL, University of Connecticut, and Woods Hole Oceanographic Institution (Fairall et al., 2003;Edson et al., 2013). PSL also measured significant wave height and period with a 1-dimensional downward looking RIEGL laser altimeter mounted on the bow mast.

The ship's rosette-mounted CTD was intermittently deployed off the starboard main deck for comparison to the uCTD, Wave Gliders, SWIFTs, and NTAS moorings. Water was collected from the Niskin bottles for analysis of the isotopic composition of oxygen and hydrogen. In addition, the ship had an underway seawater sampling system consisting of a thermistor SBE38 located at the intake valve on the hull and a thermosalinograph SBE45 located inside the ship. These sensors produced underway measurements of temperature and conductivity (salinity) from water sampled at ~5.3 m below the surface. The values recorded may be representative of seawater properties shallower in depth due to an unknown amount of mixing along the hull of the ship that is dependent on currents, ship speed, and waves. The ship also had a 75 kHz acoustic Doppler current profiler (ADCP) for the measurement of currents at depths greater than ~ 17 m.

UW deployed an underway CTD (uCTD) for the measurement of conductivity (salinity), temperature, and pressure (depth) to assess variability in the upper 60 to 130 m of the water column (Mojica and Gaube, 2020). The uCTD was

https://doi.org/10.5194/essd-2020-331
Preprint. Discussion started: 17 November 2020

deployed off the starboard aft quarter. Initially, the probe was lowered by hand with line pre-measured to 50 m. Casts were completed more frequently and with an electric winch after the NTAS mooring work was done which freed up deck space. During Leg 2, a cast with the ship's CTD was conducted every day at 13:00 (Jan. 31, Feb. 1 and 2) or 17:00 (Feb. 3, 8, and 9) shortly after a uCTD cast. These casts were used to correct the uCTD conductivity data which had a small offset due to interference from the sensor guard. A transect of intensive uCTD data was collected when the ship transited from NTAS (S1) to S2 on Jan. 18. While at S2, uCTD casts were conducted every 1 to 4 hrs. In addition, uCTD casts were conducted every 2 hrs during the majority of Leg 2 when the ship was stationary. The frequency of uCTD sampling increased to every 10 min between 13:00 and 15:15 on Feb. 9 to study heaving of periodic internal waves located at the base of the mixed layer (60-80 m depth) and for 7 hrs at the end of Leg 2 on Feb. 11 and 12 as the ship transited across a strong SST front in the upwind direction. uCTD casts were also performed when deploying or recovering the SWIFTs and Wave Gliders for comparison purposes.

2.6. Wave Glider measurements

Two Wave Gliders (serial numbers 245 and 247) operated by APL-UW were deployed within 15 minutes of each other on Jan. 9 (Fig. 1a and Table 2). The Wave Gliders greatly increased the sampling of spatial inhomogeneities in atmospheric and oceanic properties as well as bulk air-sea fluxes in the study area (Thomson and Girton, 2017;Thomson et al., 2018). The deployment occurred on the transit to NTAS approximately 45 NM to the southwest of the buoy with the intent of leaving the Wave Gliders in the water throughout the length of the cruise. They were remotely piloted from shore via an online portal to cross gradients in SST and ocean currents. Data were available in near real time which helped guide their course. The Wave Gliders were equipped with surface meteorological sensors (bulk winds, air temperature, relative humidity, pressure, and longwave and shortwave radiation), sky cameras, wave motion sensors, downward looking ADCPs for currents, and CTDs at 1 and 8 m depth for conductivity (salinity) and temperature measurements at 1 and 8 m depth. Measurements were collected during 20-min bursts every 30 min. Final data products are 60-min averages of high-resolution raw data within each hour, time-stamped at the beginning of the hour. Instrumentation onboard the Wave Gliders is listed in Table 7.

Wave Glider 245 was recovered, repaired, and redeployed on Jan 30. Telemetered data suggested that the humidity sensor had malfunctioned. When recovered, it was found that the radiometers and their entire mounting pole were gone, water was inside the data logger housing, the Airmar meteorological sensor and light were broken, and the Vaisala meteorological sensor was destroyed. The radiation measurements lasted approximately one week into the deployment. The Wave Glider was redeployed with spare Vaisala and Airmar meteorological sensors but no radiometer. Wave Glider 245 was recovered for the final time on Feb. 7 because it was experiencing navigation problems that could have endangered the vehicle. Wave Glider 247 sampled from Jan. 9 to Feb. 11. On Jan. 31, Wave Glider 247 was inspected with the ship at close range after finding Wave Glider 245 damaged the day before. The meteorological sensors were found to be in good condition but the radiometers had detached and were being

https://doi.org/10.5194/essd-2020-331
Preprint. Discussion started: 17 November 2020

dragged by wires on the port side of vehicle. A small boat was deployed to clip the radiometer wires and take the instruments back to the ship.

Table 7. Instrumentation onboard the Wave Gliders for the measurement of atmospheric and seawater parameters. Data were collected during bursts lasting 20 min at the top of each hour. Measurements were collected during 20-min bursts every 30 min. Final data products are 60-min averages of high-resolution raw data within each hour and time-stamped at the beginning of the hour.

Instrument	Measured quantity	Height (+) Depth (-) (m)	Raw sampling interval
Airmar 200WX	Wind velocity (true and relative), GPS position, COG, SOG, magnetic heading, temp, pressure, pitch and roll	+1.3	1 sec
Vaisala WXT530	Wind velocity, air temperature, pressure, relative humidity, rain rate	+1	1 sec
Kipp Zonen CMP3 pyranometer	Short wave radiation (300-2800 nm)	+1	5 sec
Kipp Zonen CGR3 pyrgeometer	Long wave radiation (4200-4500 nm), temperature of sensor	+1	5 sec
GPSWaves/Microstrain 3DM-GX3-35 GPS/AHRS	Directional (2D) wave spectra, and standard bulk wave parameters of height, period, direction	0	0.25 sec
Aanderaa 4319	Conductivity, temperature	-0.24	2 sec
RDI Workhorse Monitor 300kHz ADCP	Ocean current profiles with 4 m vertical resolution	data between -6 to -100 m	1 second pings, ensemble averages recorded every 2 min
Seabird GPCTD+DO	Conductivity, temperature, depth, dissolved O2	-8 m	10 sec

2.7. SWIFT measurements

Drifting with ocean currents and winds, the SWIFTs (Surface Wave Instrument Floats with Tracking) offered a Lagrangian view of the near-surface ocean and atmospheric properties, ocean waves and currents, bulk air-sea fluxes, and cloud features (Thomson, 2012;Thomson et al., 2019). Instrumentation onboard SWIFTs v4 and v3 is listed in Tables 8 and 9, respectively. Six SWIFT drifters were deployed in two SE-NW lines across gradients in SST and ocean surface currents – once during Leg 1 and once during Leg 2. These gradients were identified with satellite MUR v4 SST daily plots and the ship's underway thermistor, thermosalinograph, and ADCP. Two version 3 (serial number 16 and 17) and four version 4 (serial number 22, 23, 24, and 25) SWIFTs were deployed. All had bulk meteorological sensors (winds, air temperature and pressure on all models, plus relative humidity on the v4 models), sky cameras, and CTD sensors at 0.3 m depth for measuring temperature and conductivity (salinity). The v3 models also had conductivity and temperature sensors at 1.1 m depth. The v3 SWIFTs measured ocean turbulence in the upper 0.62 m. The v4 SWIFTs measured ocean turbulence in the upper 2.64 m. Both versions had ADCPs that measured vertical profiles of currents down to 20 m. The SWIFTs sampled high resolution bursts of data for 8 min at the top of each hour. These data were archived on board the vehicle for final processing once recovered. The 8-min data segments and platform location were also averaged and reported via Iridium satellite

https://doi.org/10.5194/essd-2020-331
Preprint. Discussion started: 17 November 2020

telemetry each hour for monitoring purposes. SWIFT locations were also tracked in real time using the AIS ship traffic system (local VHF radio signals). The SWIFTs were deployed for 8 days during Leg 1 (Jan. 14 to 22) and 13 days during Leg 2 (Jan. 30 to Feb. 11).

Table 8. Instrumentation onboard the version 4 SWIFTs (serial numbers 22, 23, 24, 25) for the measurement of atmospheric and seawater parameters. Measurements were collected during 8-min bursts at the beginning of each hour. Final data products are 8-min averages of high-resolution raw data, time-stamped at the beginning of each hour.

Instrument	Measured quantity	Height (+) Depth (-) (m)	Raw sampling interval
Vaisala WXT530	Wind velocity, air T, barometric pressure, relative humidity, rain rate	0.5	1 sec
Camera	320 x 240 JPEG cloud images	0.2	4 sec
SBG Ellipse GPS/AHRS	Directional (2D) wave spectra, and standard bulk wave parameters of height, period, direction	0	0.2 sec
Nortek Signature 1000 ADCP with AHRS	Turbulent kinetic energy dissipation rate profiles with 0.04 m vertical resolution	-0.3 to -2.64	0.25 sec
	Ocean current profiles with 0.5 m vertical resolution	-0.35 to -20	0.25 sec
	3-D motion and heading data	0	0.25 sec
Aanderaa 4319	Conductivity (salinity), temperature	-0.3	2 sec

Table 9. Instrumentation onboard the version 3 SWIFTs (serial numbers16 and 17) for the measurement of atmospheric and seawater parameters. Measurements were collected during 8-min bursts at the beginning of each hour. Final data products are 8-min averages of high-resolution raw data and time-stamped at the beginning of the hour.

Instrument	Measured quantity	Height (+) Depth (-) (m)	Raw sampling interval
Airmar 200WX	Wind velocity, GPS position, COG, SOG, magnetic heading, air temperature and pressure, pitch and roll	0.8	1 sec
Camera	320 x 240 JPEG cloud images	0.2	4 sec
GPSWaves/Microstrain 3DM-GX3-35 GPS/AHRS	Directional (2D) wave spectra, standard bulk wave parameters of height, period, direction	0	0.25 sec
Nortek Aquadopp ADCP	Turbulent kinetic energy dissipation rate profiles with 0.04 m vertical resolution	-0.02 to -0.62	0.25 sec
	Ocean current profiles with 0.5 m vertical resolution	-0.65 to -20	0.25 sec
Aanderaa 4319	Conductivity (salinity), temperature	-0.50	2 sec
Aanderaa 4319	Conductivity (salinity), temperature	-1	2 sec

https://doi.org/10.5194/essd-2020-331
Preprint. Discussion started: 17 November 2020

Open Access Earth System Science Data Discussions

2.8. Saildrone measurements

NOAA sponsored two Saildrones for the ATOMIC campaign to obtain high quality multiscale air-sea fluxes (Zhang et al., 2019) in two different regimes. Both were launched from Bridgetown, Barbados on Jan. 12, 2020. Saildrone SD1063 focused on the large ocean eddies southeast of BCO, where the North Brazil Current Rings propagate northwestward toward Barbados. Saildrone 1064 sampled in Trade Wind Alley along the leg between BCO and NTAS. In addition, Saildrone 1064 coordinated sampling with the *RV Ronald H. Brown*, remote sensing from research aircrafts, NTAS, Wave Gliders, and SWIFTs. Saildrones 1063 and 1064 were equipped to measure near surface ocean temperature and salinity, upper-ocean current profiles (6m-100m), surface air temperature, humidity, pressure, wind direction and speed, wave height and period, short- and long-wave radiation, and cloud images (Table 10). This system enabled calculation of the bulk latent heat flux and direct turbulent fluxes of momentum and sensible heat. Six thermistors were strapped on the keel to measure the surface layer stratification. Onboard data processing included averaging and motion correction. One-minute averages (5-minute average for ADCP current) were telemetered in real time, while high resolution data were downloaded after the Saildrones returned to U.S. During the 1-month ATOMIC intensive observation period of Jan. 12 to Feb. 12, Saildrone 1064 continuously measured air-sea interaction processes between BCO and NTAS and sailed 1777 nautical miles. After ATOMIC, the Saildrones continued their observations until July 16 and then sailed back to the U.S. arriving in Newport, RI on August 30, 2020.

Three additional Saildrones were piloted by a NASA-funded effort. These data and their details are posted at https://podaac.jpl.nasa.gov/dataset/SAILDRONE_ATOMIC, https://doi.org/10.5067/SDRON-ATOM0.

2.9. RAAVEN UAS measurements

The University of Colorado operated a small remotely-piloted aircraft system (RAAVEN) from Morgan Lewis Beach on the northeastern shore of Barbados between Jan. 24 and Feb. 16. The miniFlux payload flew onboard the RAAVEN UAS (de Boer et al., 2020). Flights conducted during this campaign targeted the thermodynamic and kinematic structure of the lower atmosphere, with sampling occurring between the surface and 1 km altitude. The vast majority of the flights were focused on the sub-cloud layer, with extended sampling conducted at cloud base and a sequence of set altitudes within the sub-cloud layer. Included in these flights were regular sampling intervals at 20 m above the ocean surface to collect information on turbulent surface fluxes of heat and momentum. Most flights were conducted in the near-coastal zone between 0 and 2 km from the coastline. MiniFlux sensors included a multihole pressure probe (MHP); fine-wire array; IR thermometers; pressure, temperature and humidity sensors similar to those used in radiosondes and dropsondes; redundant pressure, temperature, and humidity probes; and an inertial navigation system.

https://doi.org/10.5194/essd-2020-331
Preprint. Discussion started: 17 November 2020

Table 10. Instrumentation onboard the NOAA sponsored Saildrones. 1-minute averages (5-minute average for ADCP current) were telemetered in real time except where noted below. Final data products are 1-min averages of high resolution raw data.

Instrument	Measured quantity	Height (+) Depth (-) (m)	Raw sampling interval
Gill WindMaster 1590-PK	Wind velocity (true and relative), GPS position, COG, SOG, magnetic heading, temp, pressure, pitch and roll	+5.2	0.1 sec
Rotronic Hygroclip 2	Air temperature, relative humidity	+2.3	1 sec
SPN1 Delta-T Sunshine pyranometer	Short wave radiation	+2.8	0.2 sec
Eppley Precision Infrared Radiometer (PIR)	Long wave radiation, temperature	+0.8	1 sec
VectorNav VN300 DualGPS aided IMU (Wing)	GPS position, COG, SOG, magnetic heading, pitch and roll (motion correction for WindMaster and SPN1)	+2.575	0.05 sec
VectorNav VN300 DualGPS aided IMU (Hull)	Wave height and wave period and motion correction for ADCP currents	+0.34	0.05 sec
LICOR LI-192SA	Photosynthetically Active Radiation (PAR)	+2.6	1 sec
WET Labs ECO-Fluorometer	Chlorophyll-a (experimental)	-0.5	1 sec
RBR C.T.ODO.chl-a	Conductivity, temperature, dissolved O2, Chl-a (experimental)	-0.53	Inductive CTD
Teledyne RDI Workhorse 300kHz ADCP	Ocean current profiles	-6 to -100	1 sec, 5 min avg. sent via telemetry
Heitronics CT15.10	Skin seawater temperature (experimental)	0	1 sec
Vaisala PTB 210	Barometric pressure	+0.2	1 sec
4 Cameras	Cloud image	Upward, sideways, downward	Every 5 min, telemetered every 30 min
Seabird SBE57 temperature loggers	Temperature	-0.3, -0.6, - 0.9, -1.2, -1.4, -1.7	1 sec, 1 min avg. not telemetered
Seabird SBE37 CTD+DO	Conductivity, temperature, depth, dissolved O2	-0.5	Pumped, burst sampled 10 sec for 1min/5 min

2.10. SVPS drifter measurements

Though not deployed from the *R/V Ronald H. Brown*, the ATOMIC field campaign and its archive also includes a dataset of 9 SVPS type surface ocean drifters deployed by NOAA AOML (Surface Velocity Program Salinity, (Centurioni et al., 2015;Hormann et al., 2015)). These were deployed from the EUREC^{4}A ship *RV L'Atalante* 50 to 150 NM from the South American coast, between 6^{o}N and 10^{o}N, the so-called Boulevard de Tourbillons (Eddy Boulevard), where North Brazil Current Rings translate northwestward (Fig. 1b). The purpose of these drifters was to measure air-sea interaction, ocean properties, and atmospheric variability amidst ocean eddies and low-salinity plumes from a Lagrangian perspective. During ATOMIC the SVPS drifters measured air pressure and relative wind

https://doi.org/10.5194/essd-2020-331
Preprint. Discussion started: 17 November 2020

at 0.5 m height. They also measured ocean salinity and temperature (0.3, 5, 10 m depth, with a duplicate T sensor at 0.3 m), and ocean velocity representative of water located between 11-19 m depth and centered at 15 m. The drifter was equipped with a drogue centered at 15 m in the form of a long vertically-oriented holey sock. The drogue's full extent spanned a depth of 11.34 m to 18.66 m. Therefore, currents calculated from the drifter location are representative of currents between these depths. Bulk wind stress and the bulk drag coefficient were estimated from these data using COARE 3.6. Data records began at different times and locations to sample different ocean features. Four drifters started on Jan. 23, 1 drifter on Jan. 26, 4 drifters on Feb. 2, and 1 drifter on Feb 4. The drifters exited the ATOMIC/EUREC4A region on about Apr. 29, which marks the end of this archived ATOMIC dataset. After this date, data were still being reported from some sensors and can be accessed by contacting the PI (Table 11). The drifter sensors sampled every 90 sec and then computed averages over 30 min. The averaged data were transmitted to land via satellite telemetry. The position and time data were instantaneous every 30 min. Ten total drifters were deployed but GPS did not work on one so that dataset is not posted.

2.11. BACO aerosol measurements

Size resolved CCN number concentrations were measured with a custom-made DMA for size selection connected to a DMT CCNC-100 and a GRIMM 5.412 CPC. Aerosol number size distributions were made with a SMPS (GRIMM 5.420) with a diameter range of 0.10 to 1.094 µm. Measurements were made from an isokinetic aerosol inlet located at roughly 47 m.a.s.l.

3. Overview of meteorological and surface seawater conditions sampled

During ATOMIC, the *RV Ronald H. Brown* primarily operated in Trade Wind Alley, north of 12.5°N between ~56°W and NTAS (Fig. 1a). During the boreal winter, near-surface winds from the northeast carry air masses from NTAS to BCO in about 1.5 d. Positioning the *RV Ronald H. Brown* in Trade Wind Alley allowed for sampling of atmosphere and ocean conditions from the surface in between NTAS and BCO. Winds were fairly steady throughout the cruise with an average speed (10 m) of 8.3 ± 2.1 m sec^{-1} and direction of 70 ± 21° (Fig. 4a). Air temperature (10 m) ranged between 22.7 and 27.9°C and averaged 25.7 ± 0.61 °C. RH averaged 71 ± 4.7% (Figure 4b). Radiosondes launched within Trade Wind Alley revealed dryer conditions in the lower and middle troposphere compared to observations made to the south in the Boulevard de Tourbillons which paralleled the coast of South America (Fig. 1b). Stephan et al. (2020) attribute the difference to more frequent periods of a deep moist layer and deeper convection to the south.

Rain rate was measured by three instruments during the cruise located at different places on the ship. Two Parsivel disdrometers were located on the port rail on the O3 deck, an ORG-815 DA optical range gauge was located on the mast tower, and a Vaisala WXT536 was mounted on top of an aerosol sampling van on the O2 deck. Although instruments and locations were not identical, a coherent picture of rain occurrence emerges with frequent events

https://doi.org/10.5194/essd-2020-331
Preprint. Discussion started: 17 November 2020

Figure 4. Time series of bow mast measurements of a) wind speed and direction, b) air temperature and relative humidity all adjusted to 10 m height using the COARE 3.6 bulk model. Also shown are c) rain rate measured with three different instruments, d) dust and elemental carbon mass concentration for particles with aerodynamic diameters less than 10 µm, and e) skin seawater temperature from the sea snake and downwelling longwave radiation.

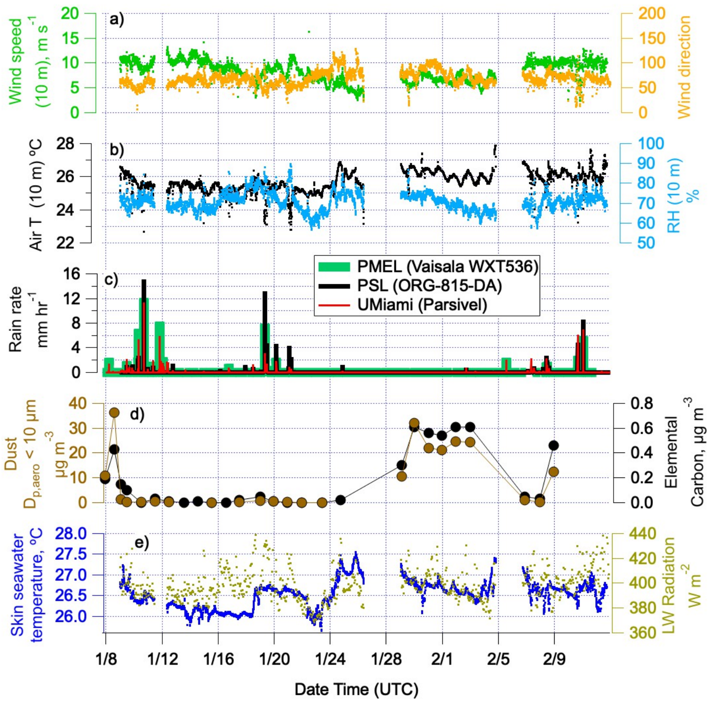

between Jan. 9 and 12; Jan. 19 and 21; and Feb. 8, 10, and 11 (Figure 4c). January rain events were associated with a stationary front extending along 20°N from the east into Barbados. February events occurred as an Atlantic ridge progressed eastward inducing strong winds and scattered showers.

One unique feature of the atmospheric conditions during ATOMIC was the occurrence of high concentrations of dust in the boreal winter. Dust concentrations have long been documented to increase each summer in the Caribbean due to transport from Africa (Prospero and Mayol-Bracero, 2013). A layer of warm, dry air above the marine boundary, known as the Saharan Air Layer (SAL), extends from Africa to North America during the summer which leads to relatively long aerosol residence times and efficient transport of dust between the two continents (Petit et al., 2005;Carlson and Prospero, 1972). Factors contributing to dust transport to the Caribbean during the winter are not as well understood but have been shown to correlate with the southward movement of the Intertropical Convergence Zone (ITCZ) which affects near-surface northeasterly winds over North Africa (Doherty et al., 2012). As a result, the SAL occurs at lower altitudes and more southern latitudes in the winter (Tsamalis et al., 2013;Liu et al., 2012).

Filter measurements of particulate Al, Si, Ca, Fe, and Ti onboard the *RV Ronald H. Brown* were used to derive dust concentrations (Malm et al., 1994). As shown in Fig. 4d, elevated dust concentrations were observed at the beginning of Leg 1 (Jan 8 00:00 to Jan. 9 12:00) and two more times during Leg 2 (Jan. 29 12:00 to Feb. 3 19:00 and Feb. 9 00:00 to Feb. 11 12:00). Dust concentrations were still elevated when aerosol sampling was halted on Feb. 3 and Feb. 11. Elemental carbon (EC) concentrations were enhanced during these same periods indicating transport of biomass burning along with the dust. The NASA Fire Information for Resource Management System (FIRMS) satellite product indicated a wide swath of fires over North Africa during January and February of 2020 (https://earthdata.nasa.gov/earth-observation-data/near-real-time/firms).

The ATOMIC study area was characterized by warmer skin seawater temperatures nearer to Barbados (west of ~55°W) due, in part, to the North Brazil Current (NBC) that transports South Atlantic warm water along the coast of Brazil and into the northern hemisphere, separating from the coast around 6° to 8°N. Occasionally the NBC curves back on itself and pinches off warm eddies that move further north and into the Caribbean Sea (Fratantoni and Glickson, 2002). The coolest skin seawater temperatures were encountered in the vicinity of the NTAS and MOVE operations on the most northeastern portion of the cruise track between Jan. 12 and 16 (Fig. 1a and Fig. 4e). A second period of low skin seawater temperatures coincided with sustained relatively low longwave downwelling radiation on Jan. 22 and 23 (Fig. 4e) although causes of the low temperatures have yet to be determined.

4. Inter-platform data comparisons

Times when the *RV Ronald H. Brown* was in close proximity to or upwind of other sampling platforms are listed in Table 3. These periods provide the potential for inter-platform comparisons for data quality checks or scientific purposes. Inter-platform comparisons reported here include 1) NTAS moorings and the ship (seawater and atmospheric parameters), 2) Saildrone 1064 and the ship (seawater and atmospheric parameters), 3) BCO and the ship (atmospheric parameters), 4) BACO and the ship (aerosol properties), and 5) BCO, the ship, and RAAVEN UAS (cloud base height). These comparisons were done to evaluate consistencies in the measurements. Resolving identified inconsistencies will be the subject of future research.

4.1. Comparison of seawater parameters

4.1.1. Onboard RHB. No significant offsets or biases were found among the independently calibrated subsurface temperature measurements onboard *RV Ronald H. Brown*. Measurements from the ship's CTD, uCTD, PSL sea snake, and ship's underway thermosalinograph and thermistor were similar. After correcting for a small bias found in the uCTD salinity, no significant difference was found among the different salinity measurements recorded.

https://doi.org/10.5194/essd-2020-331
Preprint. Discussion started: 17 November 2020

4.1.2. NTAS – RHB. Four CTD casts with the ship's rosette were conducted to compare to the NTAS moorings' upper ocean measurements between Jan. 12 and 15. The ship was 3 NM southwest of the NTAS-18 mooring anchor on Jan. 12 and 13 and 3.8 NM northwest of the NTAS-17 mooring anchor on Jan. 15 (Table 3 and Fig. 5a). With an anchor radius watch circle of ~ 2 NM for each buoy, the ship and buoys were within 0.25 to 3 NM of each other. NTAS measurements of temperature and salinity at 5 depths (10, 25, 40, 55, and 70 m) are overlaid onto data from the ship's CTD in Figure 5. Absolute differences (NTAS – RHB) in temperature are less than 0.1°C for all depths of the three casts conducted on Jan. 12 and 13 except for the last cast during that period (Fig. 5j). For the most part, the salinity comparisons show good agreement for the Jan. 12 and 13 casts with absolute differences at depths between 10 and 40 m being less than 0.03 (Fig.5 k). Exceptions occurred at lower depths due to strong vertical gradients.

The comparison from Jan. 15 shows significant differences for both temperature (Fig. 5j) and salinity (Fig. 5k) likely due to horizontal gradients. Satellite derived sea surface salinity and SST for this day indicate that NTAS and the ship were located in a frontal region with the ship in warmer and saltier surface water to the north of NTAS. The sign of the absolute differences (NTAS – RHB) in temperature and salinity varied with depth. The ship's ADCP revealed vertical structure in the currents consistent with the sign of observed absolute differences at the surface versus lower depths.

4.2. Comparison of atmospheric parameters

4.2.1. NTAS – RHB

Atmospheric parameters (temperature, relative humidity, specific humidity, wind speed, pressure, rain rate, and longwave downwelling radiation) measured onboard the NTAS buoys and the *RV Ronald H. Brown* were compared when the platforms were within 3 NM of each other between Jan. 10 and 15 (Table 3). Measurements from NTAS-17 and NTAS-18 were combined into one data set for the comparison. Based on 1-hr averaged data, 59 samples were available for comparison.

Wind speed, temperature, and specific humidity from both platforms were adjusted to a height of 10 m. Absolute differences (NTAS – RHB) were positive for temperature (Fig. 6a), RH (Fig. 6b), specific humidity (Fig. 6c), and wind direction (Fig. 6d). These differences, however, were within either reported accuracies of the instrumentation or within the range reported for a previous 24-hr *RV Ronald H. Brown* – Stratus 4 buoy comparison (Colbo and Weller, 2009). Absolute differences (NTAS – RHB) were negative for wind speed, pressure, rain rate, and longwave downwelling radiation although all differences were within accuracies of the instrumentation or within the range reported by Colbo and Weller (2009).

Figure 5. Comparison of upper ocean measured parameters from the NTAS 18 mooring and the *RV Ronald H. Brown* on Jan. 12, 13, and 15 with a) location of NTAS-18 mooring anchor. The NTAS buoys were about 2 NM downwind (SW) of the anchor so the CTD and mooring measurements were within 0.5 to 3 NM of each other. Also shown are b – e) temperature, f – i) salinity, and j – k) absolute differences and root mean square differences (rmsd) for temperature and salinity, respectively. Number of samples = 4.

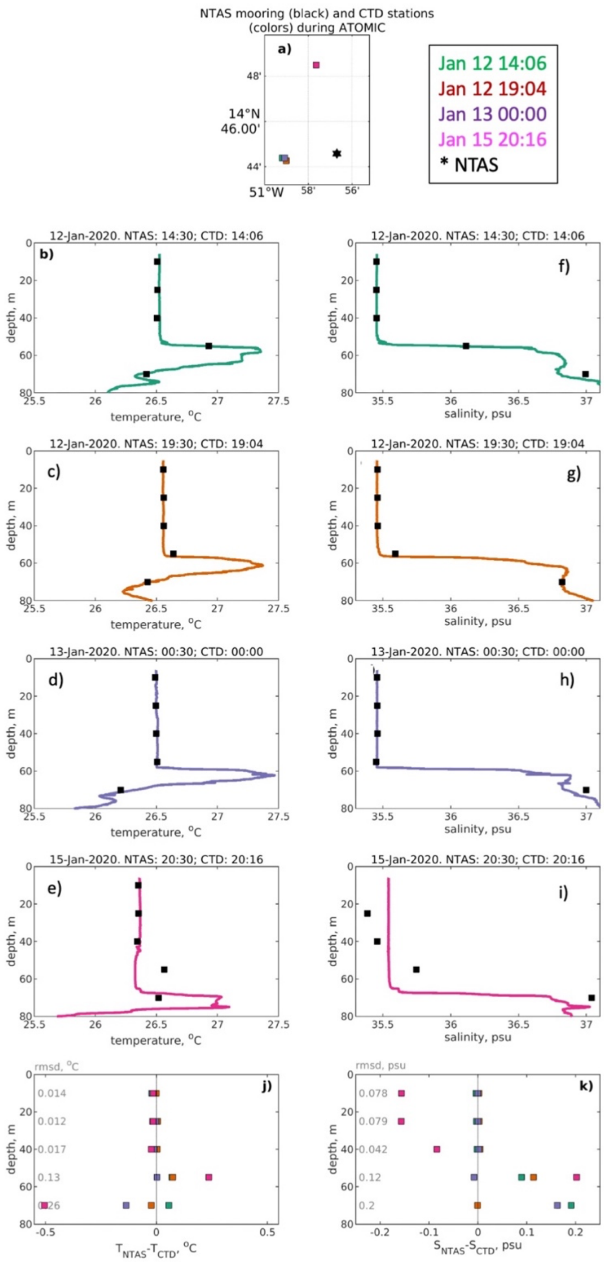

https://doi.org/10.5194/essd-2020-331
Preprint. Discussion started: 17 November 2020

Figure 6. Comparison of meteorological parameters measured onboard the NTAS buoy and the *RV Ronald H. Brown* (RHB) when the platforms were between 0.25 and 3 NM apart between Jan. 10 and Jan. 15 including a) atmospheric temperature (10 m), b) relative humidity (10 m), c) specific humidity (10 m), d) wind direction, e) wind speed (10 m), f) atmospheric pressure (10 m), g) rain rate, and h) longwave downwelling radiation. The averaged of absolute differences (NTAS – RHB) and root mean square differences (rmsd) are reported in the inset table. Number of samples based on 1 hr averaged data = 59.

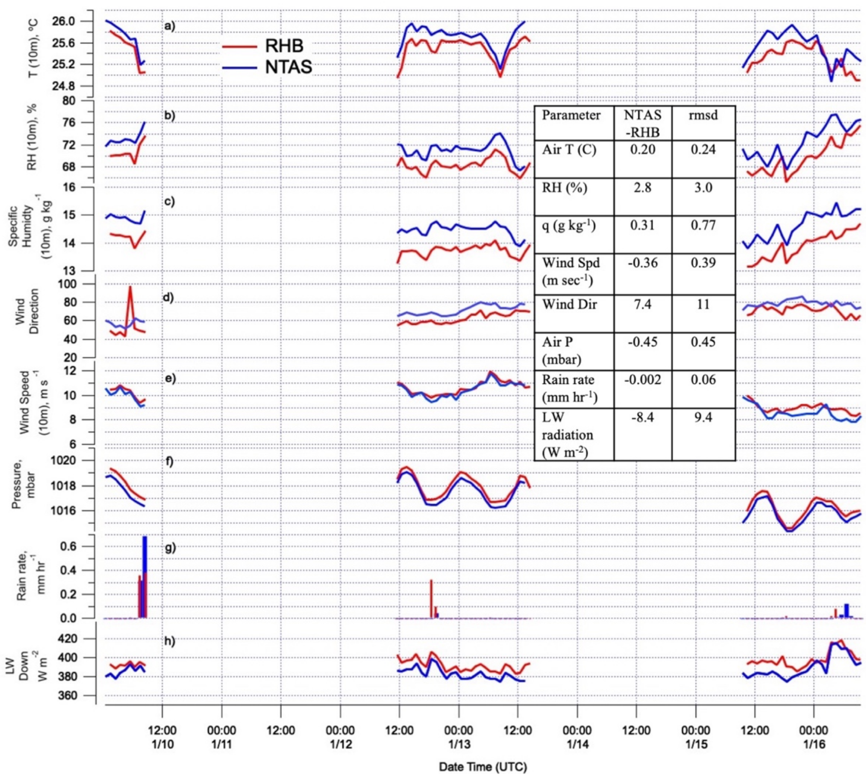

Parameter	NTAS -RHB	rmsd
Air T (C)	0.20	0.24
RH (%)	2.8	3.0
q (g kg^{-1})	0.31	0.77
Wind Spd (m sec^{-1})	-0.36	0.39
Wind Dir	7.4	11
Air P (mbar)	-0.45	0.45
Rain rate (mm hr^{-1})	-0.002	0.06
LW radiation (W m^{-2})	-8.4	9.4

4.2.2. BCO – RHB

The Barbados Cloud Observatory (BCO) is located at Deebles Point on the eastern coast of Barbados. Atmospheric parameters (temperature, RH, wind direction and speed, pressure, and rain rate) were compared between BCO and the ship during the period the ship was 20 NM east and upwind of the observatory (Jan. 24 18:20 to Jan. 25 23:40) (Table 3). BCO meteorological sensors were located at 30 m.a.s.l. and were not adjusted to a height of 10 m. Based on 10-min averaged data, 177 samples were available for comparison.

The average of the absolute difference (BCO – RHB) in temperature over the entire period was larger than instrumental accuracies (Fig. 7a). The largest difference was observed after 12:00 UTC (08:00 local) indicating relatively more warming of the sensor and/or atmosphere at BCO due to diurnal heating of the land surface. Even

https://doi.org/10.5194/essd-2020-331
Preprint. Discussion started: 17 November 2020

with differences in temperature, RH values from the two platforms agreed well with the exception of the end of the period. The ship observed an abrupt change in temperature and RH on Jan. 25 at 19:30 (Fig. 7a,b) suggesting that the platforms were in different air masses. Wind direction agreed well between platforms (Fig. 7c) but the average of the absolute differences (BCO – RHB) in wind speed (Fig. 7d) and pressure (Fig. 7e) were larger than instrumental uncertainties. One rain event occurred during the comparison. It was observed on Jan. 24 on the ship and 30 minutes later at BCO with observed rain rates of 1.2 and 3.5 mm hr^{-1}, respectively (Fig. 7f).

Figure 7. Meteorological parameters measured during the *RV Ronald H. Brown* (RHB) and the Barbados Cloud Observatory (BCO) comparison (Jan. 24 18:20 to Jan. 25 23:40) when RHB was 20 NM due east of BCO. Parameters include a) atmospheric temperature, b) relative humidity (RH), wind direction, wind speed, atmospheric pressure, and rain rate. The average of the absolute differences (BCO – RHB) and root mean square differences (rmsd) are reported in the inset table. BCO meteorological sensors were located at 30 m.a.s.l. and were not adjusted to a height of 10 m. Number of samples based on 10 minute averaged data = 177.

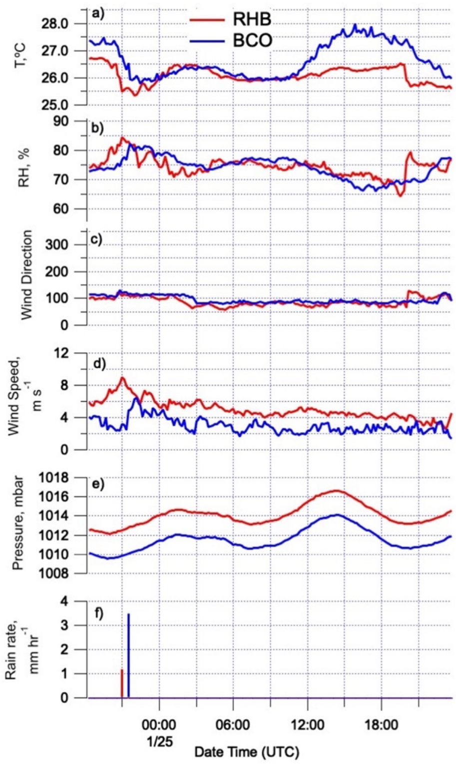

Parameter	BCO – RHB	rmsd
Air T (C)	0.53	0.74
RH (%)	-0.39	3.4
Wind Dir	5.5	14
Wind Spd (m sec^{-1})	-2.0	2.3
Air P (mbar)	-2.6	2.6
Rain rate (mm hr^{-1})	2.3*	

*n = 1 (Jan. 20 event with BCO shifted 0.5 hr earlier)

4.2.3. SD1064 – RHB

Saildrone 1064 and the *RV Ronald H. Brown* were within 0.7 to 3.6 nm of each other between Feb. 8 and 10. Based on 10 min averaged data, 663 samples were available for the comparison. Air temperature, RH, and wind speed

https://doi.org/10.5194/essd-2020-331
Preprint. Discussion started: 17 November 2020

adjusted to 10 m were used for the comparison. Skin seawater temperature was measured at a depth of 0.05 m on the Saildrone and from the ship's Sea Snake. On average, skin seawater temperature agreed within 0.01°C, atmospheric temperature within 0.12 °C, and RH within 1.9%. – all within the uncertainty of the measurements or within the agreement observed between the NTAS buoy and the ship (see Sect. 4.2.1.) (Fig. 8a, b, c). At the end of the comparison, ship measured seawater temperature at 0.05 m decreased, atmospheric temperature decreased, and RH increased while Saildrone observed parameters remained steady even though the platforms were within 0.8 nm of each other. These differences indicate the fine scale nature of structural differences in surface oceanic and lower atmospheric conditions.

On average, agreement for wind direction and wind speed was not within instrumental uncertainties or the agreement observed between the NTAS buoy and the ship due to spikes in the ship's measurements not observed by the Saildrone (Fig. 8d, e). Atmospheric pressure agreed well with an absolute difference (SD0164 – RHB) of -0.27 mbar (Fig. 8f). The absolute difference in downward long wave radiation (SD0164 – RHB) was 4.4 W m^{-2}, indicating a systemic offset (Fig. 8g).

Figure 8. Comparison of parameters measured onboard Saildrone 1064 (SD1064) and *RV Ronald. H. Brown* (RHB) when the platforms were within 0.7 to 3.6 NM of each other between Feb. 8 and 10. Parameters include a) SST (SD at -0.05 m and RHB Sea Snake), b) air temperature (10 m), c) RH (10 m), d) wind direction, e) wind speed (10 m), f) atmospheric pressure (10 m), and g) longwave downwelling radiation. Absolute differences (SD1064 – RHB) and root mean square differences (rmsd) are reported in the inset table. Number of samples based on 10 min averaged data = 663.

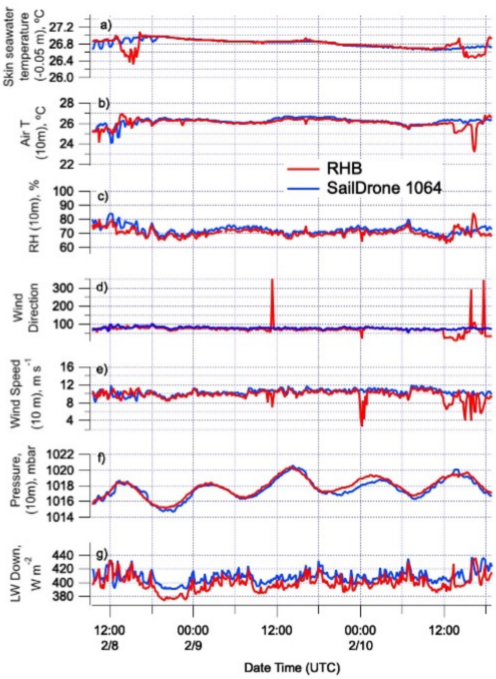

Parameter	SD1064 – RHB	rmsd
SST (C)	0.01	0.19
Air T (C)	0.12	0.45
RH (%)	1.9	3.6
Wind Spd (m sec^{-1})	0.55	1.5
Wind Dir (m sec^{-1})	13	2.2
Air P (mbar)	-0.27	0.49
LW Radiation (W m^{-2})	4.4	14

https://doi.org/10.5194/essd-2020-331
Preprint. Discussion started: 17 November 2020

4.3. Comparison of aerosol and cloud parameters

4.3.1. BACO – RHB – aerosol parameters

The Barbados Atmospheric Chemistry Observatory (BACO) is located at Ragged Point, 400 m across a cove from BCO. Total particle number concentration (CN), cloud condensation nuclei (CCN) concentration at 0.4% supersaturation, and particle number size distributions were compared between BACO and the ship when the ship was 20 NM east and upwind of BACO (Jan. 24 18:20 to Jan. 25 23:40) (Table 3). Details on the *RV Ronald H. Brown* aerosol measurements are shown in Table 5 and details on CCN calibration and measurements are provided in Quinn et al. (2019). Details on BACO CCN calibrations and measurements are provided in Pöhlker et al. (2018).

CN and CCN concentrations are shown in Fig. 9 from the time when BACO measurements began (Jan. 22 00:16) to when the ship's measurements ended (Jan. 9 20:20). Based on CN concentrations below 300 cm^{-3}, both platforms encountered clean marine conditions until ~Jan. 29 at 12:00. Subsequent enhanced concentrations of both CN and CCN correspond to periods when dust and biomass burning reached the study area after transport from Africa (Fig. 4d) as observed in related earlier studies (Wex et al., 2016). The coherence of CN and CCN between the platforms, even when separated by 4 degrees of longitude, indicates a broadscale dust event.

Figure 9. Aerosol parameters measured onboard the *RV Ronald H. Brown* (RHB) and at Barbados Atmospheric Chemistry Observatory (BACO) for the the period of overlapping measurements. The rectangle indicates the comparison period (Jan. 24 18:20 to Jan. 25 23:40) when RHB was 20 NM due east of BACO. Parameters include a) total particle number condensation (CN) and b) cloud condensation nuclei concentration (CCN) measured at 0.4% supersaturation. The average of the absolute differences (BACO – RHB) and root mean square differences (rmsd) for the comparison period are reported in the inset table. Number of samples = 5.

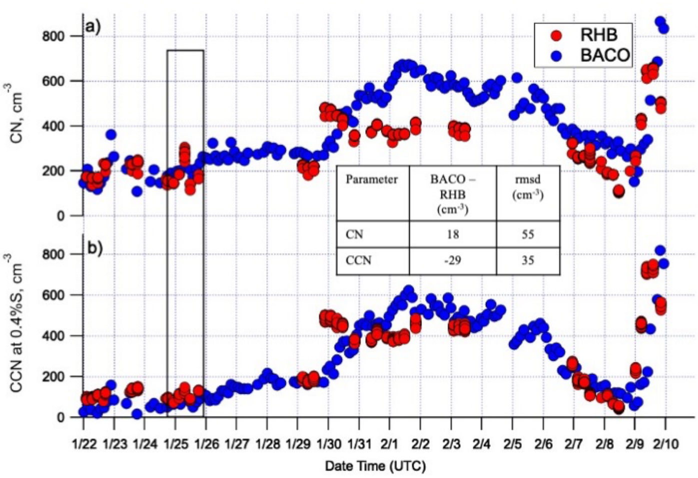

https://doi.org/10.5194/essd-2020-331
Preprint. Discussion started: 17 November 2020

The comparison when the ship was upwind of BACO is indicated by the rectangle in Fig. 9. CCN concentrations were compared at a single supersaturation (S = 0.4%) which limited the number of samples to 5. The absolute difference (BACO – RHB) was 18 cm^{-3} for CN, which is less than 10% of the average CN concentration during the comparison period and less than measurement uncertainties (Rose et al., 2008) (Fig. 9a). The difference for CCN was -29 cm^{-3} indicating the ship observed more CCN at S = 0.4% than BACO (Fig. 9b). However, this difference is within reported measurement uncertainties for mono- and polydisperse CCN measurements.

Shipboard and BACO size distributions averaged over the length of the comparison were bimodal with Aitken modal diameters of ~40 nm for both the ship and BACO and 130 and 170 nm for the accumulation mode for the ship and BACO, respectively (Fig. 10).

Figure 10. Comparison of aerosol number size distribution measured onboard the *RV Ronald H. Brown* (RHB) and at the Barbados Atmospheric Chemistry Observatory (BAC)) during the comparison period (Jan. 24 18:20 – Jan. 25 23:40) when RHB was 20 NM to the east of BACO.

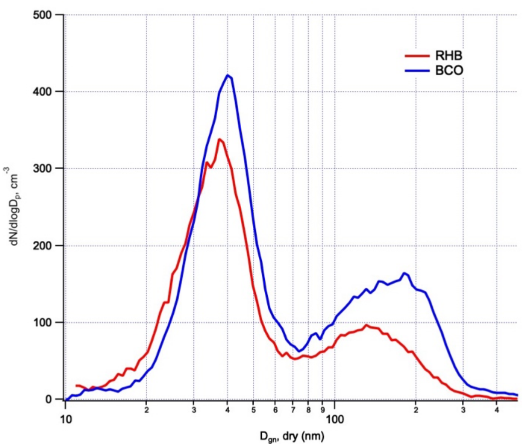

4.3.2. BCO – RHB – cloud base height

Cloud base height (CBH) was derived from three different measurements onboard the *RV Ronald H. Brown* – LCL calculated from the stitched together RHB – BCO radiosonde record (equation 1), the ceilometer, and the microDop lidar (Fig. 11a). Fifth and 10th percentile values of the lowest cloud scattered return were averaged over 10 min intervals of the ceilometer and lidar data, respectively. The choice of percentile levels was tested to reduce inclusion of scattering at the surface made by rain and scattering aloft from horizontally-sheared cloud edges. Higher altitude ceilometer and lidar values that remain in this time series are not representative of cloud base due to the presence and scattering by sheared edges or detrained portions of clouds that are separated horizontally from the locations of cloud base. Dilution of surface parcels with drier air could also contribute to rising heights of the cloud base. Lowest values from both the ceilometer and lidar track well with the LCL values derived from the radiosondes.

https://doi.org/10.5194/essd-2020-331
Preprint. Discussion started: 17 November 2020

Open Access Earth System Science Data Discussions

Figure 11. Comparison of Cloud Base Height (CBH) for a) legs 1 and 2 onboard *RV Ronald H. Brown* (RHB) based on LCL calculated from the stitched together RHB – BCO radiosonde record (equation 1), the ceilometer, and the Doppler lidar and b) for the RHB – BCO comparison period (Jan. 24 18:20 – Jan. 25 23:40) based on the BCO ceilometer, LCL from BCO radiosondes, the RHB ceilometer and microDop lidar, and the RAAVEN UAS flown from Morgan Lewis (30 km north of BCO). Locations of the RAAVEN launch site, BCO, and RHB are shown in c). The averaged of the absolute differences and root mean square differences (rmds) are shown in the table inset relative to the RHB lidar-derived CBH. N indicates number of samples used in the comparison. *rmsd for RHB ceilometer – RHB microDop lidar with CBH greater than 1000 m removed from comparison.

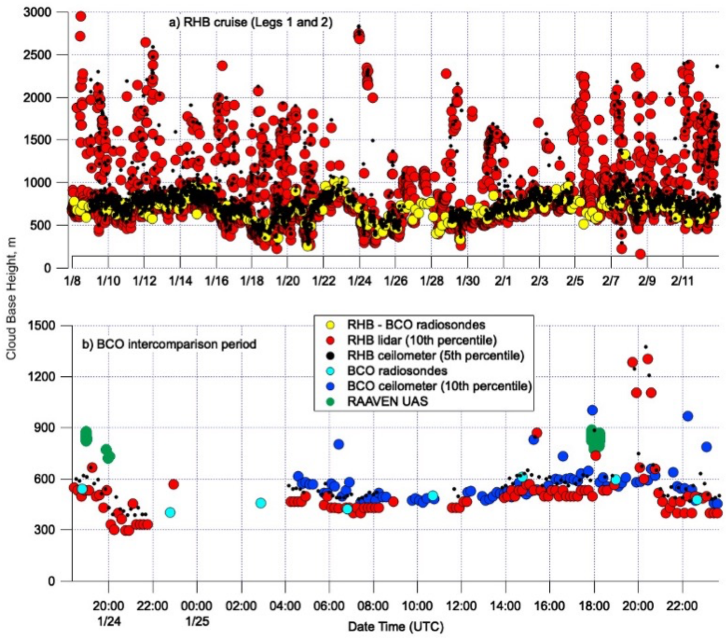

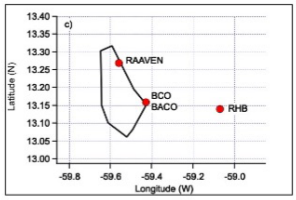

Comparison to RHB lidar	Absolute difference (m)	rmsd (m)	N
RHB cruise Legs 1 and 2			
RHB-BCO LCL from sondes	-137	15	197
RHB ceil	0.66	360 73*	3139
BCO comparison period			
BCO LCL from sondes	-37	88	6
RHB ceil	68	81	91
BCO ceilometer	35	200	56
RAAVEN	260	640	6

On average, the absolute difference between the LCL and lidar values (RHB-BCO LCL – RHB lidar) is -137 m due to lidar scattering off of slightly higher altitude clouds. On average, the absolute difference between the RHB ceilometer and microDop lidar (RHB ceilometer – RHB lidar) is 0.66 m indicating good agreement while the rmsd value of 360 m reveals larger point to point differences. If CBHs from the ship's ceilometer and microDop lidar are limited to values less than 1000 m, rmsd decreases to 73 m.

For the BCO comparison period (Jan. 24 18:20 – Jan. 25 23:40), CBHs were compared from the ship's ceilometer and microDop lidar, BCO's ceilometer and LCLs from radiosondes, and the RAAVEN UAS miniFlux payload (Fig. 11b). The RAAVEN UAS flew from the eastern side of Barbados, 30 km north of BCO. Locations of the RAAVEN launch site, BCO, and ship during the comparison are shown in Fig. 11c. Absolute differences in average values between the BCO ceilometer and RHB microDop lidar (BCO ceilometer – RHB microDop lidar) and BCO LCLs and RHB microDop lidar (BCO LCL – RHB microDop lidar) are around 35 m or 7% of the average sonde-derived CBH. The absolute difference in average values between the RHB ceilometer and RHB microDop lidar (RHB

https://doi.org/10.5194/essd-2020-331
Preprint. Discussion started: 17 November 2020

ceilometer – RHB microDop lidar) is slightly higher at 68 m. RAAVEN values are considerably higher with an absolute difference (RAAVEN miniFlux – RHB microDop lidar) of 260 m. This difference could be due to the RAAVEN flight pattern which was nearer to land than the ship, however, RAAVEN values are also higher than those observed at BCO. Alternatively, it could be related to finer-scale horizontal and vertical variability in boundary layer structure not readily-resolved by the measurements.

5. Data availability

All ATOMIC data sets discussed are publicly available at the NOAA PSL ATOMIC ftp server (ftp://ftp2.psl.noaa.gov/Projects/ATOMIC/data/) (Quinn et al., 2020). Point of contact information and links to the data sets are provided in Table 11. In addition, data have been submitted to NOAA's National Center for Environmental Information (https://www.ncei.noaa.gov/) for Digital Object Identifiers (DOIs). The data will be permanently and publicly available on the PSL ftp server and NCEI.

A readme file (README_ATOMIC_DATA.pdf) is available at ftp://ftp2.psl.noaa.gov/Projects/ATOMIC/data/ which describes the file structure of the ATOMIC folder and the content of the single files.

All of the datasets included in the discussion have been quality-controlled based on procedures implemented by the individual research teams. Versioning also is based on protocols put in place by individual research teams. Details can be found in the references listed in Table 11. Data are CF compliant. File name structure is:

<campaign_id>_<project_id>_<platform_id>_<instrument_id>_<variable_id>_<time_id>_<version_id>.nc.

An example for data collected from the ceilometer on the *RV Ronald H. Brown* is as follows. The name of the data and link are:

EUREC4A_ATOMIC_RonBrown_Ceilometer_10min_20200109_20200212_v1.0.nc.

Metadata are embedded in the individual .nc files for each data set.

https://doi.org/10.5194/essd-2020-331
Preprint. Discussion started: 17 November 2020

Open Access Earth System Science Data Discussions

Table 11. Summary of data sets, links to data sets, point of contact information, and references for data collected onboard the *RV Ronald H. Brown*, NTAS, Wave Gliders, SWIFTs, NOAA and NASA operated Saildrones, and RAAVEN UAS during ATOMIC. Links in the table are for the ftp server (ftp://ftp2.psl.noaa.gov/Projects/ATOMIC/data/). (Quinn et al., 2020). Data have been submitted to NOAA's National Center for Environmental Information (https://www.ncei.noaa.gov/) for Digital Object Identifiers (DOIs) and for permanent archiving. The data will be permanently and publicly available on the PSL ftp server, and NCEI.

Platform	**Data set**	**Data Link (preliminary FTP site location while NCEI DOIs are still being minted)**	**Point of Contact**	**Reference**
All	ATOMIC	ftp://ftp2.psl.noaa.gov/Projects/ATOMIC/data/	elizabeth.thompson@noaa.gov	Zuidema (2020)
RHB	Air-sea fluxes, ship navigation/location information, meteorological parameters, solar and infrared radiation, rain rate, subskin seawater T, skin seawater T (NOAA PSL)	ftp://ftp2.psl.noaa.gov/Projects/ATOMIC/data/rhb/met_sea_flux_nav/	elizabeth.thompson@noaa.gov	Fairall et al. (1997);Fairall et al. (2003);Edson et al. (2013)
	ROSR skin seawater T (NOAA PSL)	ftp://ftp2.psl.noaa.gov/Projects/ATOMIC/data/rhb/ROSR/	elizabeth.thompson@noaa.gov	
	Ceilometer (NOAA PSL)	ftp://ftp2.psl.noaa.gov/Projects/ATOMIC/data/rhb/ceilometer/	elizabeth.thompson@noaa.gov	
	Disdrometer (rain rate, drop number, equivalent radar reflectivity) (U Miami)	ftp://ftp2.psl.noaa.gov/Projects/ATOMIC/data/rhb/disdrometer/	pzuidema@rsmas.miami.edu	Zuidema et al. (2012)
	W-band radar (U Miami in partnership with NOAA PSL)	ftp://ftp2.psl.noaa.gov/Projects/ATOMIC/data/rhb/W-band-radar/	pzuidema@rsmas.miami.edu elizabeth.thompson@noaa.gov	
	Sky camera (U Miami)	https://www.dropbox.com/sh/zejurecda70bilq/AABlLWgrEv1MDZ07yIE5TgWWa?dl=0	pzuidema@rsmas.miami.edu	
	M-AERI skin seawater T, air humidity and temperature (U Miami)	ftp://ftp2.psl.noaa.gov/Projects/ATOMIC/data/rhb/M-AERI/	pzuidema@rsmas.miami.edu gszczodrak@rsmas.miami.edu	Szczodrak et al. (2007)
	Doppler lidar (NOAA CSL)	ftp://ftp2.psl.noaa.gov/Projects/ATOMIC/data/rhb/doppler_lidar/	alan.brewer@noaa.gov	Schroeder et al. (2020)
	Picarro water vapor isotopes (OSU/NCAR)	ftp://ftp2.psl.noaa.gov/Projects/ATOMIC/data/rhb/Picarro/	david.noone@auckland.ac.nz	
	Picarro seawater isotopes	ftp://ftp2.psl.noaa.gov/Projects/ATOMIC/data/rhb/seawater_isotopes/	david.noone@auckland.ac.nz	
	Meteorological and aerosol properties (NOAA PMEL)	ftp://ftp2.psl.noaa.gov/Projects/ATOMIC/data/rhb/atmos-chem/	derek.coffman@noaa.gov	Bates et al. (2002)
	Radiosondes (OSU)	https://doi.org/10.5194/essd-2020-174	simon.deszoeke@oregonstate.edu	Stephan et al. (2020)
	Underway CTD, uCTD (APL-UW)	ftp://ftp2.psl.noaa.gov/Projects/ATOMIC/data/rhb/UCTD/	kdrushka@apl.uw.edu	Mojica and Gaube (2020)
	Ship rosette CTD (APL-UW)	ftp://ftp2.psl.noaa.gov/Projects/ATOMIC/data/rhb/CTD/	kdrushka@apl.uw.edu	
	Ship ADCP (APL-UW)	ftp://ftp2.psl.noaa.gov/Projects/ATOMIC/data/rhb/ADCP/	kdrushka@apl.uw.edu	
NTAS mooring	Meteorological parameters, air-sea fluxes, solar and infrared radiation; ocean currents, waves, conductivity, salinity, and temperature (WHOI)	ftp://ftp2.psl.noaa.gov/Projects/ATOMIC/data/NTAS/	aplueddemann@whoi.edu	Weller (2018)
Wave Gliders	Air-sea fluxes, meteorological parameters, radiation; ocean currents, turbulence, waves, conductivity, and temperature (APL-UW)	ftp://ftp2.psl.noaa.gov/Projects/ATOMIC/data/wavegliders/	jthomson@apl.washington.edu	Thomson and Girton (2017)
SWIFT drifter	Air-sea fluxes, meteorological parameters, radiation; ocean currents, turbulence, waves,	ftp://ftp2.psl.noaa.gov/Projects/ATOMIC/data/swift_drifters/	jthomson@apl.washington.edu	Thomson et al. (2019)

https://doi.org/10.5194/essd-2020-331
Preprint. Discussion started: 17 November 2020

	conductivity, and temperature (APL-UW)			
Saildrones (NOAA)	Air-sea fluxes, meteorological parameters, radiation; ocean currents, waves, conductivity, and temperature (NOAA PMEL)	ftp://ftp2.psl.noaa.gov/Projects/ATOMIC/data/saildrones_noaa/	dongxiao.zhang@noaa.gov	Zhang et al. (2019)
Saildrones (NASA)	Air-sea fluxes, meteorological parameters, radiation; ocean currents, waves, conductivity, and temperature (NASA)	https://doi.org/10.5067/SDRON-ATOM0	cgentemann@faralloninstitute.org	
SVPS drifters	Meteorological and ocean parameters, wind stress (NOAA AOML)	ftp://ftp2.psl.noaa.gov/Projects/ATOMIC/data/svp-s_drifters/	greg.foltz@noaa.gov	Centurioni et al. (2015);Hormann et al. (2015)
RAAVEN miniFlux	Met parameters (Univ. Colorado)	ftp://ftp2.psl.noaa.gov/Projects/ATOMIC/data/CU-RAAVEN/	gijs.deboer@noaa.gov	de Boer et al. (2020)

As an example, the metadata for Cloud Base Height is:

long_name: cloud base height
standard_name: cloud_base_altitude
units: km
coverage_content_type: thematicClassification
instrument: ceilometer_instrument
platform: RonBrown
coordinates: time
cell_methods: time: point
valid_range: 0.0, 7.0
actual_range: 0.28, 6.86975
_FillValue: -9999.0
comment: Computed as the 5th percentile of cloud1, the height of first cloud layer detected, from 15 sec raw data over this time period.

6. Summary

During ATOMIC, *in situ* and remote sensing measurements of oceanic and atmospheric properties and air-sea fluxes were made from the *RV Ronald H. Brown.* In addition, the NTAS mooring, radiosondes, SWIFTs, and Wave Gliders were deployed. Descriptions of the instrumentation onboard the ship and the deployed assets are provided along with the sampling strategy and day-to-day events. Atmospheric and oceanic conditions encountered during the cruise are described. Also detailed is how to access to all data collected. Comparisons were conducted with the NTAS moorings, Saildrone 1064, BCO, BACO, and the RAAVEN UAS. Data from inter-platform comparisons are presented to assess consistency in data sets. Resolving identified inconsistencies will be the subject of future research. The intention of the paper is to advance widespread use of the data by the ATOMIC and broader research communities.

Author contributions. P.K.Q. prepared the paper with the help of all co-authors. E.T. prepared data sets for archival on the PSL ftp server and at NCEI. D.J.C. prepared data for inclusion in the paper's figures. All authors participated in collecting and analyzing ATOMIC data.

Competing Interests. The authors declare that they have no competing interests.

Acknowledgements. We thank the crew of the *RV Ronald H. Brown* for their enthusiastic help and cooperation throughout the ATOMIC cruise and Dr. Edmund Blades and Peter Sealey for technical support at the BACO site. NOAA's Climate Variability and Predictability Program provided funding under NOAA CVP NA19OAR4310379, GC19-301, and GC19-305. The Joint Institute for the Study of the Atmosphere and Ocean (JISAO) supported this study under NOAA Cooperative Agreement NA15OAR4320063. Additional support was provided by the NOAA's Uncrewed Aircraft Systems (UAS) Program Office, NOAA's Physical Sciences Laboratory, and NOAA AOML's Physical Oceanography Division. The NTAS project is funded by the NOAA's Global Ocean Monitoring and Observing Program (CPO FundRef number 100007298), through the Cooperative Institute for the North Atlantic Region (CINAR) under Cooperative Agreement NA14OAR4320158. We would like to thank Dr. David Farrell of the Caribbean Institute for Meteorology and Hydrology (CIMH) for his assistance with the organization of this campaign and Dr. Sandy Lucas of NOAA's Climate Program Office for her efforts that made ATOMIC and related outreach programs a success. This is PMEL contribution number 5172.

https://doi.org/10.5194/essd-2020-331
Preprint. Discussion started: 17 November 2020

References

Banner, M. L., and Morison, R. P.: Refined source terms in wind wave models with explicit wave breaking prediction. Part I: Model framework and validation against field data, Ocean Modelling, 33, 177 - 189, 2010.

Bates, T. S., Coffman, D. J., Covert, D. S., and Quinn, P. K.: Regional marine boundary layer aerosol size distributions in the Indian, Atlantic and Pacific Oceans: A comparison of INDOEX measurements with ACE-1, ACE-2, and Aerosols99, J. Geophys. Res. Atmos., 107, 10.1029/2001JD001174, 2002.

Bigorre, S. P., and Galbraith, N. R.: Sensor performance and data quality control, in: Observing the Oceans in Real Time, edited by: Venkatesan, R., Tandon, A., D'Asaro, E., and Atmanand, M. A., Springer International, 243 - 261, 2018.

Bolton, D.: The Computation of Equivalent Potential Temperature, Monthly Weather Review, 108, 1046 - 1053, 1980.

Bony, S., Stevens, B., Frierson, D. M. W., Jakob, C., Kageyama, M., Pincus, R., Shepherd, T. G., Sherwood, S. C., Siebesma, A. P., Sobel, A. H., Watanabe, M., and Webb, M. J.: Clouds, circulation, and climate sensitivity, Nature Geosci., 8, 261 - 268, 2015.

Bony, S., Stevens, B., Ament, F., Bigorre, S., Chazette, P., Crewell, S., Delanoe, J., Emanuel, K., Farrell, D., Flamant, C., Gross, S., Hirsch, L., Karstensen, J., Mayer, B., Nuijens, L., Ruppert, J. H., Sandu, I., Siebesma, P., Speich, S., Szczap, F., Totems, J., Vogel, R., Wendisch, M., and Wirth, M.: EUREC4A: A field campaign to elucidate the couplings between clouds, convection and circulation, Surveys in Geophysics, 38, 1529 - 1568, 2017.

Carlson, T. N., and Prospero, J. M.: The large-scale movement of Saharan air outbreaks over the northern equatorial Atlantic, Journal of Applied Meteorology, 11.2, 283 - 297, 1972.

Centurioni, L. R., Hörmann, V., Chao, Y., Reverdin, G., Font, J., and Lee, D.-K.: Sea surface salinity observations with Lagrangian drifters in the tropical North Atlantic during SPURS: Circulation, fluxes, and comparisons with remotely sensed salinity from Aquarius, Oceanography, 28, 96 - 105, 2015.

Colbo, K., and Weller, R. A.: Accuracy of the IMET Sensor Package in the Subtropics, J Atmos Ocean Tech, 26, 1867 - 1890, 2009.

de Boer, G., Calmer, R., Cox, C. J., Borenstein, S., Rhodes, M., Choate, C., Hamilton, J., Argrow, B., and Intrieri, J.: Measurements from the University of Colorado RAAVEN Remotely-Piloted Aircraft System during ATOMIC, Earth System Science Data, in preparation, 2020.

Doherty, O. M., Riemer, N., and Hameed, S.: Control of Saharan mineral dust transport to Barbados in winter by the Intertropical Convergence Zone over West Africa, J. Geophys. Res. Atmos., 117, 10.1029/2012JD017767, 2012.

Edson, J. B., Jampana, V., Weller, R. A., Bigorre, S., Plueddemann, A. J., and Fairall, C. W.: On the exchange of momentum over the open ocean, J Phys Oceanogr, 43, 1589 - 1610, 2013.

Espy, J. P.: Essays on Meteorology, No. IV: North East Storms, Volcanoes, and Columnar Clouds, Journal of the Franklin Institute, 22, 239 - 246, 1836.

Fairall, C. W., Bradley, E. F., Rogers, D. P., Edson, J. B., and Young, G. S.: Bulk parameterization of air–sea fluxes in TOGA COARE, J. Geophys. Res. Atmos., 101, 3747 - 3767, 1996.

Fairall, C. W., White, A. B., Edson, J. B., and Hare, J. E.: Integrated Shipboard Measurements of the Marine Boundary Layer, J Atmos Ocean Tech, 14, 338 - 359, 1997.

Fairall, C. W., Bradley, E. F., Hare, J. E., Grachev, A. A., and Edson, J. B.: Bulk parameterization of air-sea fluxes: Updates and verification for the COARE algorithm, J Climate, 16, 571 - 591, 2003.

Fratantoni, D. M., and Glickson, D. A.: North Brazil Current Ring Generation and Evolution Observed with SeaWiFS, J Phys Oceanogr, 32, 1058 - 1074, 2002.

Hormann, V., Centurioni, L. R., and Reverdin, G.: Evaluation of drifter salinities in the subtropical North Atlantic, J Atmos Ocean Tech, 32, 185 - 192, 2015.

Liu, D., Wang, Y., Wang, Z., and Zhou, J.: The Three-Dimensional Structure of Transatlantic African Dust Transport: A New Perspective fom CALIPSO LIDAR Measurements, Adv Meteorol, 2012, 10.1155/2012/850704, 2012.

Malm, W. C., Sisler, J. F., Huffman, D., Eldred, R. A., and Cahill, T. A.: Spatial and seasonal trends in particle concentration and optical extinction in the United States, J. Geophys. Res. Atmos., 99, 1347 - 1370, 1994.

Minnett, P., Knuteson, R. O., Best, F., and Osborne, B. J.: The Marine-Atmospheric Emitted Radiance Interferometer (M-AERI), a high-accuracy, sea-going infrared spectroradiometer, J Atmos Ocean Tech, 18, 94 - 1013, 2001.

Mojica, K., and Gaube, P.: Estimates of mixing and mixed layer depth in the Western North Atlantic, Frontiers, submitted, 2020.

Moran, K., Pezoa, S., Fairall, C. W., Williams, C., Ayers, T., Brewer, A., Szoeke, S. P. d., and Ghate, V.: A Motion-Stabilized W-Band Radar for Shipboard Observations of Marine Boundary-Layer Clouds. , Boundary Layer Meteorology, 143, 3 - 24, 2012.

Petit, R. H., Legrand, M., Jankowiak, I., Molimie, J., Asselin de Beauville, C., Marion, G., and Mansot, J. L.: Transport of Saharan dust over the Caribbean islands: Study on an event, J. Geophys. Res. Atmos., 110, 10.1029/2004JD004748, 2005.

Pincus, R., Fairall, C. W., Bailey, A., Chen, H., Chuang, P. Y., Boer, G. d., Feingold, G., Henze, D., Kazil, J., Kalen, Q. T., Leandcro, M., Lundry, A., Moran, K., Naeher, D. A., Patel, A. J., Pezoa, S., Popstefanija, I., Warnecke, J., and Zuidema, P.: Observations from the NOAA research aircraft during the ATOMIC field campaign, Earth System Science Data, in preparation, 2020.

Pöhlker, M. L., Ditas, F., Saturno, J., Klimach, T., de Angelis, I. H., Araujo, A. C., Brito, J., Carbone, S., Cheng, Y., Chi, X., Ditz, R., Gunthe., S. S., Holanda, B. A., Kandler, K., Kesselmeier, J., Konemann, T., Kruger, O. O., Lavric, J. V., Martin, S. T., Mikhailov, E., Moran-Zuloaga, D., Rizzo, L. V., Rose, D., Su, H., Thalman, R., Walter, D., Wang, J., Wolff, S., Barbosa, H. M. J., Artaxo, P., Andreae, M. O., Poschl, U., and Pohlker, C.: Long-term observations of cloud condensation nuclei over the Amazon rain forest – Part 2: Variability and characteristics of biomass burning, long-range transport, and pristine rain forest aerosols, Atmos Chem Phys, 18, 10289 - 10331, 2018.

Prospero, J. M., and Mayol-Bracero, O. L.: Understanding the transport and impact of African dust on the Caribbean Basin, Bulletin of the American Meteological Society, 94, 1329 - 1337, 2013.

Quinn, P. K., Bates, T. S., Coffman, D. J., Upchurch, L., Moore, R., Ziemba, L. D., Bell, T. G., Saltzman, E. S., Graff, J., and Behrenfeld, M. J.: Seasonal variations in western North Atlantic remote marine aerosol properties, J. Geophys. Res. Atmos., 124, 14240 - 14261, 2019.

Quinn, P. K., Thompson, E., Coffman, D. J., Baidar, S., Bariteau, L., Bates, T. S., Bigorre, S., Brewer, A., Boer, G. d., Szoeke, S. P. d., Drushka, K., Foltz, G. R., Intrieri, J., Iyer, S., Fairall, C. W., Gaston, C. J., Jansen, F., Johnson, J. E., Krüger, O. O., Marchbanks, R. D., Moran, K.,

https://doi.org/10.5194/essd-2020-331
Preprint. Discussion started: 17 November 2020

Noone, D., Pezoa, S., Pincus, R., Plueddemann, A. J., Pöhlker, M. L., Pöschl, U., Melendez, E. Q., Royer, H. M., Szczodrak, M., Thomson, J., Upchurch, L. M., Zhang, C., Zhang, D., and Zuidema, P.: Measurements from the RV Ronald H. Brown and related platforms as part of the Atlantic Tradewind Ocean-Atmosphere Mesoscale Interaction Campaign (ATOMIC), ftp://ftp2.psl.noaa.gov/Projects/ATOMIC/data/, 2020.

Rose, D., Gunthe, S. S., Mikhailov, E., Frank, G. P., Dusek, U., Andreae, M. O., and Poschl, U.: Calibration and measurement uncertainties of a continuous-flow cloud condensation nuclei ounter (DMT-CCNC): CCN activation of ammonium sulfate and sodium chloride aerosol particles in theory and experiment, Atmos Chem Phys, 8, 1153 - 1179, 2008.

Schroeder, P., Brewer, W. A., Choukulkar, A., Weickmann, A., Zucker, M., Holloway, M. W., and Sandberg, S.: A Compact, Flexible, and Robust Micropulsed Doppler Lidar, J Atmos Ocean Tech, 37, 1387 - 1402, 2020.

Smirnov, A., Holben, B. N., Slutsker, I., D.M.Giles, McClain, C. R., Eck, T. F., Sakerin, S. M., Macke, A., P.Croot, Zibordi, G., Quinn, P. K., Sciare, J., Kinne, S., Harvey, M., Smyth, T. J., Piketh, S., Zielinski, T., Proshutinsky, A., Goes, J. I., Nelson, N. B., Larouche, P., Radionov, V. F., Goloub, P., Moorthy, K. K., Matarrese, R., Robertson, E. J., and Jourdin, F.: Maritime Aerosol Network as a component of Aerosol Robotic Network, J. Geophys. Res. Atmos., 114, D06204, doi:10.1029/2008JD011257, 2009.

Stephan, C., Schnitt, S., Schulz, H., Bellenger, H., Szoeke, S. P. d., Acquistapace, C., Baier, K., Dauhut, T., Laxenaire, R., Morfa-Avalos, Y., Person, R., Quinones-Melendez, E., Bagheri, G., Bock, T., Daley, A., Guttler, J., Helfer, K. C., Los, S. A., Neuberger, A., Rottenbacher, J., Raeke, A., Ringel, M., Ritchel, M., Sadoulet, P., Schirmacher, I., Stolla, M. K., Wright, E., Charpentier, B., Doerenbecher, A., Wilson, R., Jansen, F., Kinne, S., Reverdin, G., Speich, S., Bony, S., and Stevens, B.: Ship- and island-based atmospheric soundings from the 2020 EUREC4A field campaign, Earth System Science Data, under review, 2020.

Stevens, B., Farrell, D., Hirsch, L., Jansen, F., Nuijens, L., Serikov, I., Brugmann, B., Forde, M., Linne, H., Lonitz, K., and Prospero, J. M.: The Barbados Cloud Observatory: Anchoring Investigations of Clouds and Circulation on the Edge of the ITCZ, Bulletin of the American Meteological Society, 97, 787 - 801, 2016.

Stevens, B., Bony, S., Farrell, D., Ament, F., Blyth, A., Fairall, C. W., Karstensen, J., Quinn, P. K., Speich, S., and e.t., a.: European project ElUcidating the RolE of Cloud-Circulation Coupling in ClimAte (EUREC4A), Advances, in preparation, 2020.

Szczodrak, M., Minnett, P. J., Nalli, N. R., and Feltz, W. F.: Profiling the Lower Troposphere over the Ocean with Infrared Hyperspectral Measurements of the Marine-Atmosphere Emitted Radiance Interferometer, J Atmos Ocean Tech, 24, 390 - 402, https://doi.org/10.1175/JTECH1961.1., 2007.

Thomson, J.: Wave Breaking Dissipation Observed with SWIFT Drifters, J Atmos Ocean Tech, 29, 1866--1882, 10.1175/JTECH-D-12-00018.1, 2012.

Thomson, J., and Girton, J.: Sustained Measurements of Southern Ocean Air-Sea Coupling from a Wave Glider Autonomous Surface Vehicle, Oceanography Magazine, 30, 104-109, 2017.

Thomson, J., Girton, J. B., Jha, R., and Trapani, A.: Measurements of Directional Wave Spectra and Wind Stress from a Wave Glider Autonomous Surface Vehicle, J Atmos Ocean Tech, 35, 347-363, 2018.

Thomson, J., Moulton, M., de Klerk, A., Talbert, J., Guerra, M., Kastner, S., Smith, M., Schwendeman, M., Zippel, S., and Nylund, S.: A new version of the SWIFT platform for waves,

https://doi.org/10.5194/essd-2020-331
Preprint. Discussion started: 17 November 2020

currents, and turbulence in the ocean surface layer, IEEE/OES Workshop on Currents, Waves, and Turbulence Measurements, 2019,

Tsamalis, C., Chedin, A., Pelon, J., and Capelle, V.: The seasonal vertical distribution of the Saharan Air Layer and its modulation by the wind, Atmos Chem Phys, 13, 11235 - 11257, 2013.

Vial, J., Bony, S., Dufresne, J. L., and Roehrig, R.: Coupling between lower-tropospheric convective mixing and low-level clouds: Physical mechanisms and dependence on convection scheme, Journal of Advances in Modeling Earth Systems, 8, https://doi.org/10.1002/2016MS000740, 2016.

Weller, R. A.: Observing surface meteorology and air sea fluxes, in: Observing the Oceans in Real Time, edited by: Venkatesan, R., Tandon, A., D'Asaro, E., and Atmanand, M. A., Springer International, 17 - 35, 2018.

Wex, H., Dieckmann, K., Roberts, G., Conrath, T., Izaguirre, M. A., Hartmann, S., Herenz, P., Schafer, M., Ditas, F., Schmeissner, T., Henning, S., Wehner, B., Holger-Siebert, H., and Stratmann, F.: Aerosol arriving on the Caribbean island of Barbados: physical properties and origin, Atmos Chem Phys, 16, 14107 - 14130, 2016.

Whittlestone, S., and Zahorowski, W.: Baseline radon detectors for shipborad use: Development and deployment in the First Aerosol Characterization Experiment (ACE-1), J. Geophys. Res. Atmos., 103, 16743-16751, 1998.

Zhang, D., Cronin, M. F., Meinig, C., Farrar, J. T., Jenkins, R., Peacock, D., Keene, J., Sutton, A., and Yang, Q.: Comparing Air-sea flux measurements from a new unmanned surface vehicle and proven platforms during the SPURS-2 Field Campaign, Oceanography, 32, 122 - 133, 2019.

Zuidema, P., Li, Z., Hill, R., Bariteau, L., Rilling, B., Fairall, C. W., Brewer, W. A., Albrecht, B., and Hare, J. E.: On trade-wind cumulus cold pools, Journal of Atmospheric Science, 69, 258 - 277, 2012.

Zuidema, P.: Overview of ATOMIC, in preparation, 2020.